New indolo-β-lactam hybrids as potential anticancer and anti-inflammatory agents

Saeedeh Ghaffari, Aliasghar Jarrahpour, Namik Özdemir, Jean Michel Brunel, Banafsheh Rastegari, Elham Riazimontazer, Edward Turos

New indolo-β-lactam hybrids as potential anticancer and anti-inflammatory agents

Saeedeh Ghaffari[1] · Aliasghar Jarrahpour[1] · Namik Özdemir[2] · Jean Michel Brunel[3] · Banafsheh Rastegari[4] · Elham Riazimontazer[5,6] · Edward Turos[7]

Abstract

In this work, two groups of structurally novel indolo-β-lactam hybrids were synthesized by ketene-imine [2 + 2] cycloaddition reaction. In the first series, the reaction proceeded between various selected aromatic imines and a ketene derived from indole-3-acetic acid. For the second, *N*-acetic acid indole-3-carbaldehyde was used as the ketene source in reaction with imines. The new indolo-β-lactam hybrids were obtained as exclusively the *cis* stereoisomer based on ^{1}H NMR spectroscopy and X-ray crystallography studies. These compounds were examined for anticancer and anti-inflammatory activities. Between synthesized compounds, 4b and 4o in the first series showed the most in vitro anticancer activity against HeLa, MCF7 and A549 cancer cell lines. In anti-inflammatory studies, indolo-β-lactam 4e with anti-inflammatory ratio of 85.90 and indolo-β-lactam 9k with anti-inflammatory ratio of 141.23, had the most anti-inflammatory activity than dexamethasone with anti-inflammatory ratio of 37.87, as standard. Molecular docking experiments indicate that the active compounds bind optimally to the 4nos active sites, and suggest that 4e and 9k may serve as potential inhibitors of iNOS for treatment of inflammatory disorders.

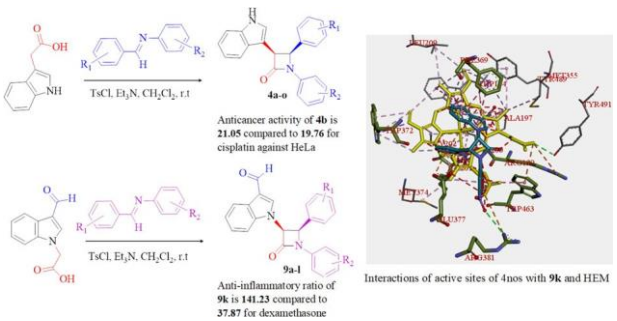

Keywords β-Lactam · Indole · Hybrid · X-ray crystallography · Anticancer · Anti-inflammatory

✉ Aliasghar Jarrahpour
jarahpor@shirazu.ac.ir

[1] Department of Chemistry, College of Sciences, Shiraz University, Shiraz 71946-84795, Iran

[2] Department of Physics, Ondokuz Mayıs University, TR-55139 Samsun, Turkey

[3] Centre de Recherche en Cancérologie de Marseille (CRCM), CNRS, UMR7258, Institut Paoli Calmettes, Aix-Marseille Université, UM 105, Inserm, U1068, Faculté de Pharmacie, Bd Jean Moulin, F-13385 Marseille, France

[4] Diagnostic Laboratory Sciences and Technology Research Center, School of Paramedical Sciences, Shiraz University of Medical Sciences, Shiraz, Iran

[5] Biotechnology Research Center, Shiraz University of Medical Sciences, Shiraz, Iran

[6] Department of Medicinal Chemistry, School of Pharmacy, Shiraz University of Medical Sciences, Shiraz, Iran

[7] Center for Molecular Diversity in Drug Design, Discovery, and Delivery, Department of Chemistry, University of South Florida, CHE 205, 4202 East Fowler Avenue, Tampa, FL 33620, USA

Introduction

The β-lactam (or azetidin-2-one) ring is an important strained heterocyclic compound with applications in microbiology and medicinal chemistry. This unique four-membered ring scaffold is a key unit in the penicillin and cephalosporin antibiotics and is the structural feature required for their bioactivity. For nearly 80 years now, the β-lactams have seen widespread use in treating bacterial infections [1–5]. In addition to antibacterial properties [6, 7], β-lactam compounds have been studied for a host of other applications [8]; including the inhibition of HIV-1 protease [9], analgesic activities [10], antimalarial activity [11], anticancer activity [12, 13], antimicrobial activity [14], anti-inflammatory [15, 16], antifungal [17] and anti-depressant activity (Fig. 1).

It has been reported that heterocyclic compounds are existed in many drug compounds. Indole is one of the most promising heterocyclic moiety due to its diverse biological activities and can be interested as a core in the drug development. Indole derivatives possess various biological applications in medicinal chemistry. Based on variety, research has engrossed the mind of organic chemists to discover new indole-based derivatives [18].

Some of the most important medicinal compounds have an indole moiety, such as indomethacin, roxindole, indalpine, delavirdine, perindopril, ondansetron, sumatriptan, tadalafil and fluvastatin, and the spectrum of activity includes anti-inflammatory [19], anti-HIV [20], anti-tubercular [21], antimalarial [22] anticonvulsant [23], antidiabetic [24], antimicrobial [25], anticancer [26], antioxidant [27, 28], antifungal [29] and antidyslipidemic effects [30] (Fig. 2).

In recent years, molecular hybridization has become of increasing interest due to the opportunity to explore new chemical space and what biological capabilities these hybrid molecules may have [31–34]. Our laboratories have reported on some of these advances as well, wherein β-lactams have been hybridized onto other pharmaceutically relevant ring systems as a means to enhance and to further explore their microbiological or cellular properties [35–38]. In this present study, indolo-β-lactam hybrids were synthesized and examined for anticancer and anti-inflammatory activities.

Results and discussion

Chemistry

In first part of this study, fifteen novel indolo-β-lactam hybrids 4a–o were synthesized by building the sensitive β-lactam ring directly onto an existing indole core via a [2 + 2] ketene-imine cycloaddition reaction. In all of these compounds, indole-3-acetic acid was used as the ketene source. A mixture of indole-3-acetonitrile (1) in methanol was refluxed for several hours in the presence of potassium hydroxide to afford indole-3-acetic acid (2) [39]. Schiff bases 3a–o were synthesized in ethanol under reflux conditions in the presence of acetic acid as catalyst. Subsequently, indole-3-acetic acid (2) was reacted with Schiff bases 3a–o in the presence of *p*-toluenesulfonyl chloride and triethylamine, in molar ratios of 1.5: 1: 1.5: 5 respec- tively, in dry CH_2Cl_2 at room temperature to produce *cis*- indolo-*β*-lactams 4a–o in yields varying from 70–93% after purification (Scheme 1 and Table 1).

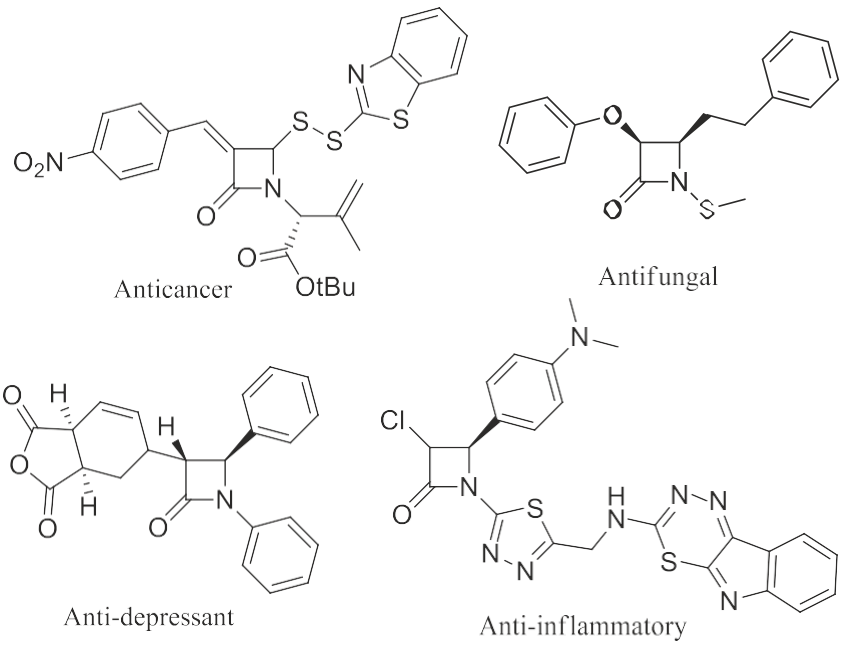

Fig. 1 Structures of some biologically active β-lactam derivatives

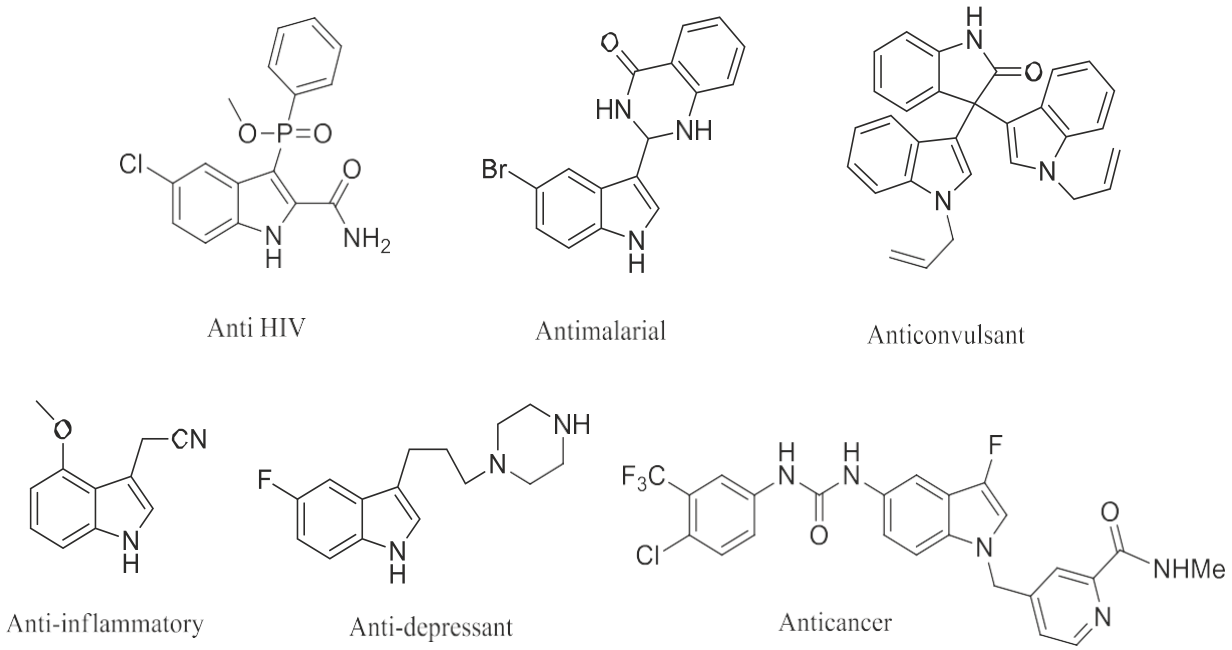

Fig. 2 Structures of some indole derivatives with diverse biological activities

In the second part, 12 new indolo-3-carbaldehyde-β-lactam hybrids 9a−l were synthesized by the Staudinger reaction. *N*-acetic acid indole-3-carbaldehyde was used as the ketene source. Indole (5) was formylated under Vilsmeier reaction conditions. In following, indole-3-carbaldehyde (6) was reacted with bromoacetic acid in the presence of calcium hydride in DMF solvent at room temperature to form *N*-acetic acid indole-3-carbaldehyde (7). Reaction of 7 with Schiff bases 8a−l, in the presence of *p*-toluenesulfonyl chloride and triethylamine in molar ratios of 1: 0.3: 1: 4 respectively, in dry CH_2Cl_2 overnight at room temperature afforded the *cis*-indolo-3-carbaldehyde-β-lactam hybrids 9a−l in yields of 54−78% after purification (Scheme 1 and Table 1).

Experiments indicate that imines with electron-releasing groups in the amine moiety and electron-withdrawing substituents in the aldehyde portion led to better results.

The structures of the indolo β-lactams 4a−o and 9a−l were established on the basis of their FTIR, ^{1}H NMR, ^{13}C NMR spectral data and elemental analysis. The stretching vibration for the carbonyl group of the azetidinone ring in β-lactam hybrids 4a−o was observed at υ 1728−1759 cm^{-1}. In β-lactams 9a−l, the stretching vibrations were at about υ 1750 cm^{-1} for azetidinone ring carbonyl group and about υ 1660 cm^{-1} for aldehyde carbonyl group. In the ^{1}H NMR spectra, the H-3 and H-4 of the β-lactam ring protons of all the compounds appeared as discrete doublets. In compounds 4a−o a signal at 164 to 168 ppm was assigned to the β-lactam carbonyl carbon in the ^{13}C NMR spectra. In β-lactams 9a−l, azetidinone ring carbonyl carbon at about 160 ppm and aldehydic carbonyl carbon at about 185 ppm were observed.

The stereochemistry of the β-lactam ring substituents was determined by ^{1}H NMR coupling constants. For the H-3 and H-4 of the azetidinone ring, ^{1}H NMR coupling con- stants are $J_{3,4} > 4.0$ Hz for the *cis* stereoisomer [11]. Also X-ray crystallography for 4b, 9c and 9f confirmed it.

X-ray crystallographic studies

In order to confirm relative stereochemistry of the β-lactams, 4b, 9c and 9f were each recrystallized from ethanol and subjected to single-crystal X-ray crystal- lography. The molecular structures of 4b, 9c and 9f with the adopted atom-labeling scheme are shown in Fig. 3. Crystal data, data collection, structure refinement details, bond distances and bond angles are obtained (see Supplementary materials).

All bond lengths and bond angles in 4b, 9c and 9f are within normal ranges [40] and comparable to those in the related compounds [41−45].

The *β*-lactam ring in 4b is planar [r.m.s deviation = 0.013 Å] and its mean plane makes dihedral angles of 12.79(15), 77.43(15) and 64.59(14)° with the methoxyphenyl, nitrophenyl and indole ring, respectively. The nitrophenyl and indole rings are in the *cis* position with respect to the *β*-lactam ring, while the methoxyphenyl ring is almost in plane with the *β*-lactam ring.

In the molecular structure of 4b, an intramolecular C─H···O contact (Fig. 3) leads to the formation of six-membered ring with a graph-set descriptor *S* (6) [46]. The crystal packing of 4b (Fig. 4) is achieved by one C─H···O and one N─H···O intermolecular hydrogen bond. In the first of these, atom C13

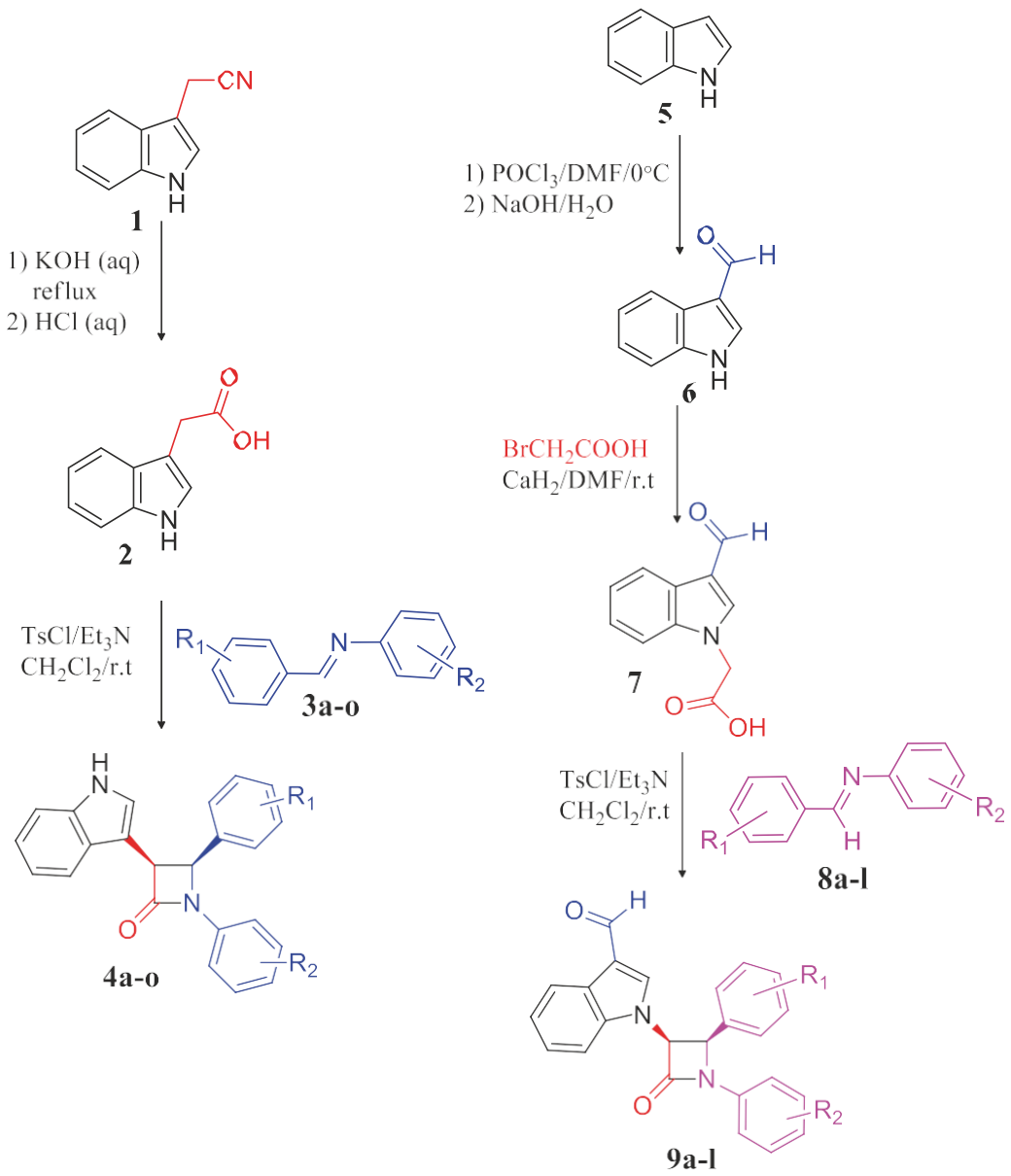

Scheme 1 Synthesis of *cis*-indolo-β-lactam hybrids 4a–o and 9a–l

in the molecule at (x, y, z) acts as a hydrogen-bond donor to atom O2 at ($-x+1$, $y-1/2$, $-z+1/2$). In the second, atom N3 in the molecule at (x, y, z) acts as hydrogen-bond donor to atom O4 in the molecule at ($x+1/2$, $-y+3/2$, $-z+1$). Full details of the hydrogen-bonding geometry are given in Fig. 4.

The structures of 9c and 9f have similar molecular dimensions. The *β*-lactam ring is planar [r.m.s deviation = 0.021 Å], and its mean plane makes dihedral angles of 15.28(10), 67.01(11) and 76.60 (9)° with the (C4-C9) phenyl, nitrophenyl and indole rings in 9c, respectively. In the case of 9f, the r.m.s deviation of the *β*-lactam ring is 0.022 Å, and the dihedral angle between its mean plane and (C4-C9) phenyl, nitrophenyl and indole rings is 12.91(13), 70.44(13) and 66.65 (11)°, respectively. In both compounds, the nitrophenyl and indole rings are in the *cis* position with respect to the *β*-lactam ring, while the (C4-C9) phenyl ring shares a common plane with the *β*-lactam ring.

Biological activities

Anticancer activity and apoptosis/necrosis analysis

In vitro anticancer activity and cytotoxicity of the synthesized compounds were examined against cervical cancer cell HeLa, breast cancer cell MCF7, lung cancer cell A549, gastric cancer cell AGS, breast cancer cell MDA-MB-468 and NIH/3T3 normal fibroblast cell line. In general, compounds 4a–o showed more activity than

Table 1 *Cis*-indolo-β-lactam hybrids 4a–o and 9a–l

Cpd	R1	R2	Isolated yield (%)	Cpd	R1	R2	Isolated yield (%)
4a	2-NO_2	4-OMe	80	9a	3-NO_2	4-OEt	78
4b	4-NO_2	4-OMe	77	9b	Anthracen-9-yl[a]	4-OMe	75
4c	2-NO_2	4-Br	70	9c	2-NO_2	4-OEt	72
4d	2-NO_2	2,4-diOMe	85	9d	2-NO_2	3,4-OCH_2CH_2O[b]	68
4e	2-NO_2	3-NO_2	77	9e	4-NO_2	4-OMe	68
4f	4-Br	4-OMe	76	9f	2-NO_2	2,4-diOMe	65
4g	4-Cl	4-OMe	75	9g	3-NO_2	4-OMe	76
4h	Anthracen-9-yl[a]	4-OMe	87	9h	4-CN	4-OMe	70
4i	2-NO_2	3,4-OCH_2CH_2O[b]	78	9i	Anthracen-9-yl[a]	4-NMe_2	78
4j	2-NO_2	4-OEt	93	9j	Anthracen-9-yl[a]	H	68
4k	3-Me	4-OEt	84	9k	2-NO_2	3-NO_2	54
4l	4-Cl	4-OEt	74	9l	Anthracen-9-yl[a]	4-NEt_2	66
4m	3,4-diOMe	4-OEt	76				
4n	3-NO_2	4-OEt	86				
4o	2-NO_2	4-I	73				

[a]Anthracene-9-carbaldehyde was used as the aldehyde source in the preparation of imine

[b]3,4-ethylendioxyaniline was used as the amine source in the preparation of imine

compounds 9a–l. In this series, 4b and 4o compounds showed the most anticancer activity against the mentioned cells. Cisplatin has been used as standard. The results are summarized in Table 2.

Annexin V/PI probe is the most commonly used method to distinguish between apoptosis, as the most important programmed cell death, from necrosis. Analyses of apoptosis/necrosis of 4b and 4o compounds on HeLa cells were conducted to examine their mechanism of neoplastic potential. The apoptosis rates were calculated as the sum of early apoptosis and late apoptosis (Fig. 5).

Anti-inflammatory activity

Inflammation is an important defence barrier of the body against infection and is indeed a biological response of the body's immune system. Closely related to this is that nitric oxide (NO) is a strong cell signaling molecule responsible for different physiological functions in mammals, including the molecule that initiates inflammatory responses. NO is a free radical formed intracellularly by the enzymatic oxidation of L-arginine to L-citrulline by a family of enzymes called nitric oxide synthases (NOSs). Under inflammatory conditions, enzymes such as inducible nitric oxide synthase (iNOS) may become activated as well, and is responsible for inflammation-related diseases [47–49]. Recently some β-lactams have shown good anti-inflammatory activity [8, 50]. So, we examined indolo-β-lactam derivatives for potential anti-inflammatory properties using the RAW 264.7 macrophage assay, an in vitro anti-inflammatory assay for murine cell line. This assay monitors the inhibitor effects on the low-grade inflammatory cascade that results in overproduction of NO in the endothelial lining of blood vessels. To evaluate each compound's anti-inflammatory potential, macrophage cultures were infected with simulated microbes (*E. coli* LPS) to induce inflammation reactions. This causes the macrophages to produce high levels of NO in the culture medium. The anti-inflammatory activity of all compounds toward iNOS was evaluated, taking Dexamethasone as the standard. The anti-inflammatory activity is determined by calculating the ratio between the cell viability and the inhibition of inflammation reactions (Table 3).

Anti-inflammatory studies showed 4a, 4c, 4e and 4o compounds in the first series and 9a and 9k compounds in the second series have anti-inflammatory potential. Compounds 4e and 9k have the most anti-inflammatory activity with anti-inflammatory ratios of 85.9 and 141.23, respectively, in comparison to the Dexamethasone, the corticosteroid drug having an anti-inflammatory ratio of 37.87.

We investigate the role of electron-donating and electron-withdrawing groups on anti-inflammatory response for compounds 4a–o and 9a–l. A clear structure-activity relationship (SAR) among these compounds was indeed found that indicates electron-withdrawing substituents on the *N*-aryl ring of the β-lactam ring enhances anti-inflammatory activity while electron-donating substituents diminishes anti-inflammation. Among the 4a–o series,

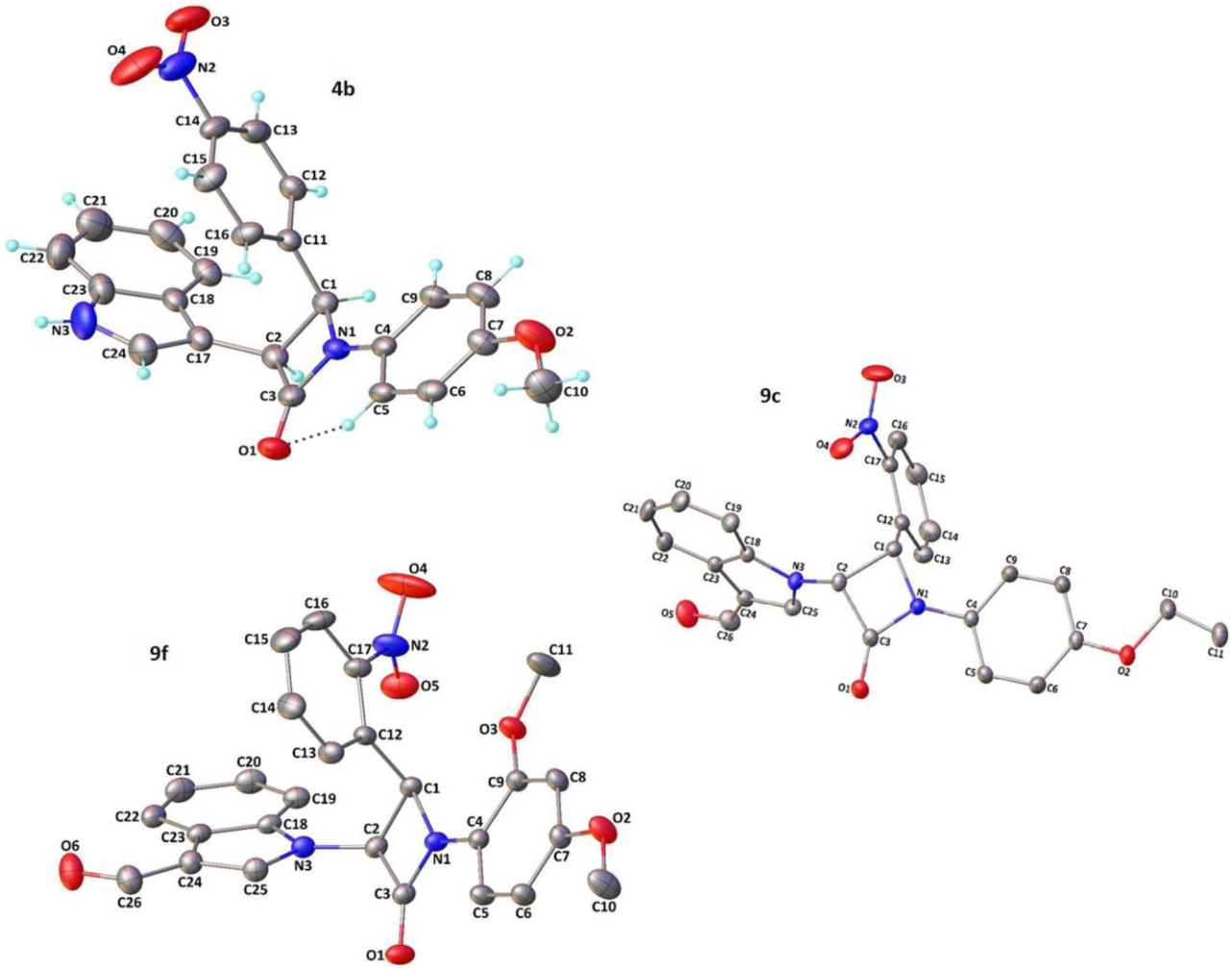

Fig. 3 Molecular structure of 4b, 9c and 9f. H atoms have been omitted for the sake of clarity in 9c and 9f. Intramolecular C─H···O contact is represented by dotted lines in 4b

compounds 4c and 4o containing a halogen and 4e bearing a electron-withdrawing substituent, afforded more anti-inflammatory activity than other compounds in this series. Conversely, compounds 4d and 4i, which both contain two electron-donating substituents, showed reduced anti-inflammatory activity. Within the 9a–l series, compound 9k having a powerful electron-withdrawing nitro substitution on the aromatic ring at the N1 position of the β-lactam ring, possessed the highest anti-inflammatory effect. However, the anti-inflammatory activity of compounds 9d and 9f, which each have two electron-donating substitution groups on the N1 position aromatic ring, was reduced. Moreover, examining the effect of aryl ring substitution at the C2 position of the β-lactam ring indicates that electron-withdrawing substituents located on this ring yields superior results compared to halogen or electron-donating groups. Among the 4a–o series, compounds 4k, 4m, and 4l containing electron-donating substituents, or a halogen, on the C2 ring diminished anti-inflammatory activity compared to when it bears a nitro group. Also, in the series of 4a–o compounds, electron-withdrawing substitution on the C2 aryl ring is more favorable in the ortho position than in the meta or para, as illustrated for 4j in comparison with 4n and 4b.

Molecular docking of indolo-β-lactams to the human nitric oxide synthase

Molecular docking is a powerful tool for evaluating the binding affinity of a ligand to its corresponding protein target, thus allowing for identification of potential drug candidates. This process involves predicting the interactions between the protein and ligand molecules and calculating the affinity of the complex. The advantages of computational molecular docking include its ability to quickly and cost-effectively screen potential inhibitors, and its accuracy in predicting and understanding how a selected molecule is likely to interact with its target protein. For these reasons,

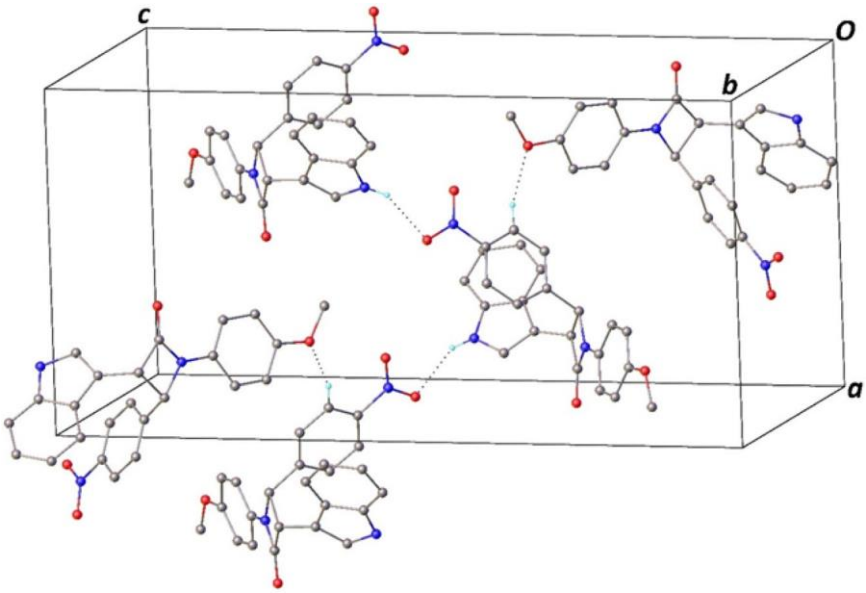

Fig. 4 Part of the crystal structure of 4b showing the intermolecular interactions and hydrogen-bonding geometry. Symmetry codes: [i] $-x+1, y-1/2, -z+1/2$; [ii] $x+1/2, -y+3/2, -z+1$

D- H···A	D- H (Å)	H···A (Å)	D···A (Å)	D- H···A (°)
C5- H5···O1	0.93	2.59	3.175(4)	121
C13- H13···O2^{i}	0.93	2.44	3.332(4)	160
N3- H3···O4^{ii}	0.86	2.20	2.976(4)	151

molecular docking can be used to help design new medicines and even identify new therapeutic targets for existing drugs. By running these simulations in silico rather than in a laboratory vessel, researchers can screen large numbers of compounds to identify those that have the highest binding affinity for the target protein whose detailed X-ray crystallographic three-dimensional coordinates are available from the Protein Data Bank (http://www.rcsb.org). We were therefore interested to use computational molecular docking to further validate the anti-inflammatory activities of the indolo-β-lactam hybrids, and to explore plausible binding interactions with the enzymatic pocket of the human inducible nitric oxide synthase (iNOS) enzyme. The receptor protein must be held rigid, while the candidate drug molecule is treated as flexible in order to bind to the receptor. The X-ray crystal structure of the human inducible nitric oxide synthase (iNOS) to the 2.25 Å resolution level, with the accession code 4nos obtained from the Protein Data Bank, provided us with the docking template. To conduct the procedure, the co-crystallized ligand from the original X-ray structure was removed and the individual β-lactams 4a–o and 9a–l were each redocked in the same region. The accuracy of docking was validated using the root-mean square deviation (RMSD), which measures the difference between the Cartesian coordinates of the ligand's atoms in the docked and crystallographic conformations, with an acceptable RMSD value of less than 2 Å. The molecular docking validation for 4nos PDB ID yielded an RMSD value of 0.50 Å. Table 3 displays the docking scores obtained from the computational experiments, which are based on the free binding energies of the synthesized compounds. In series 9a–l, due to the presence of an aldehyde group in indole-3-carbaldehyde at the C3 position of the β-lactam ring and its subsequent effect on hydrogen bonding, these compounds showed higher binding scores compared to the compound series 4a–o.

Our results showed that 4e and 9k demonstrated optimal docking scores characterized by the minimum Gibbs binding energy ($\Delta G_{bind} = -9.5$ and -9.1 kcal/mol) and dis- played the most potent in vitro anti-inflammatory activity, with anti-inflammatory ratio 85.90 and 141.23, respectively, in comparison with the reference compound dexamethasone whose anti-inflammatory ratio is 37.87 and $\Delta G_{bind} = -8.8$ kcal/mol. Figure 6 demonstrates the binding interactions between 9k and the protein's active site, 4nos PDB code. As illustrated the active site cavity of iNOS is well-suited for compound 9k.

The phenyl and indole groups of 9k exhibited π–π stacking interactions with the indole ring of Trp463 and the phenyl moiety of Phe369 (4nos), respectively. The negatively charged oxygen atom of Glu377 participated in a π-anion interaction with the phenyl ring. Additionally, one of the oxygen atoms of the nitro group in 9k formed hydrogen bonds with Ile201 and Arg381, while the indole and phenyl groups engaged in van der Waals interactions with Val352.

It seems that the presence of indole-3-carbaldehyde at the C3 position of the β-lactam ring in 9a–l series showed more potent anti-inflammatory activity than the 4a–o series, due

Table 2 IC_{50} values (μM) for compounds 4a–o and 9a–l toward mentioned cell lines (after 72 h)

Cpd	Cell lines			
	A549	MCF7	HeLa	NIH/3T3
4a	>100	>100	>100	>100
4b	49.57 ± 4.07	43.85 ± 3.45	21.05 ± 2.41	18.22 ± 3.27
4c	96.23 ± 2.91	>100	>100	>100
4d	58.52 ± 3.34	61.43 ± 4.43	53.14 ± 3.17	66.65 ± 3.39
4e	>100	>100	>100	>100
4f	84.48 ± 4.02	91.29 ± 3.67	>100	81.94 ± 3.43
4g	>100	>100	>100	>100
4h	91.08 ± 4.33	>100	>100	85.74 ± 2.66
4i	>100	>100	>100	>100
4j	88.77 ± 2.69	90.28 ± 1.77	62.95 ± 2.57	56.12 ± 4.13
4k	94.17 ± 2.90	95.42 ± 2.95	76.62 ± 4.26	71.22 ± 3.43
4l	97.49 ± 4.18	>100	93.27 ± 2.68	>100
4m	>100	>100	>100	>100
4n	>100	>100	>100	>100
4o	53.18 ± 5.02	53.11 ± 3.46	38.89 ± 2.94	32.03 ± 3.01
Cisplatin	22.94 ± 1.57	25.84 ± 2.65	19.76 ± 3.08	86.27 ± 4.08
	A549	AGS	MDA-MB-468	NIH/3T3
9a	>100	>100	>100	>100
9b	>100	>100	>100	>100
9c	>100	74.21 ± 3.61	86.68 ± 3.99	94.53 ± 2.02
9d	>100	83.29 ± 5.06	91.22 ± 2.07	78.07 ± 4.56
9e	>100	>100	>100	>100
9f	>100	>100	>100	>100
9g	>100	>100	>100	>100
9h	>100	>100	>100	>100
9i	>100	>100	>100	>100
9j	>100	>100	>100	>100
9k	>100	>100	>100	>100
9l	>100	>100	>100	>100
Cisplatin	20.67 ± 3.13	14.95 ± 2.94	20.97 ± 3.16	81.14 ± 3.67

to the aldehyde group forming a critical hydrogen bond with the HEM group. Moreover, the docking score was higher in this group. The docking study indicated that 9k exhibited good agreement with both the calculated Gibbs binding energy and our in vitro evaluation results. The findings of the molecular docking study suggest that the compounds could bind well to the active site of iNOS, which is consistent with our molecular design for iNOS.

Conclusion

In this work, two groups of new *cis*-indolo-β-lactam hybrids have been synthesized via a stereoselective [2 + 2] ketene-imine cycloaddition reaction. The ketenes needed for the cycloadditions were formed in situ using indole-3-acetic acid and *N*-acetic acid indole-3-carbaldehyde. All of the indolo-β-lactams were obtained exclusively as *cis* stereoisomers, as confirmed by ^{1}H NMR spectroscopy and also single-crystal X-ray crystallography for 4b, 9f and 9c compounds. The synthesized indolo-β-lactams were examined for selected biological activities. Anticancer studies and the MTT analysis showed the antineoplastic potential of 4b and 4o against HeLa, MCF7 and A549 cancer cell lines. Also anti-inflammatory examinations determined compounds 4a, 4c, 4e and 4o in first series and 9a and 9k in second series have potential anti-inflammatory activity against mouse immortalized macrophages (RAW 264.7 cell line) stimulated by *E. coli* LPS. Compounds 4e and 9k have the most anti-inflammatory effect with 85.9 and 141.23 respectively, which

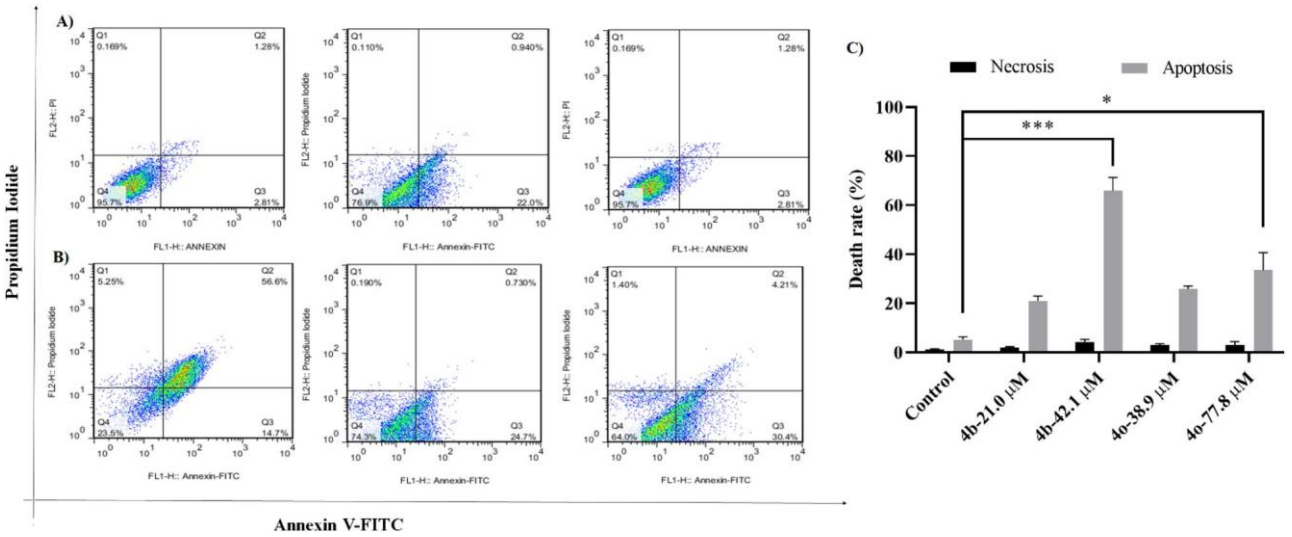

Fig. 5 The flow cytometric analysis of (A) 4b and (B) 4o complexes on HeLa cells after 24 h of incubation. The cell populations in Q1 are necrotic cells that are PI positive. Cells in the Q2 are late apoptotic cells, which are both PI and Annexin V positive. Viable cells are in Q3 that is PI or Annexin V negative. The cell populations at Q4 are Annexin V positive that are early apoptotic cells. C The death rate percentage was analyzed using nonparametric one-way ANOVA with three independent experiments. The significant *p* value is defined as follows: * value ≤ 0.05, ** value ≤ 0.01, *** value ≤ 0.001, and **** value ≤ 0.0001

are comparable to dexamethasone as standard with 37.87 anti-inflammatory ratio. Computational molecular docking experiments indicate that the most active compounds 4e and 9k effectively bind to the active site of iNOS. Our study also shows that 9k is a potential iNOS inhibitor with low toxicity. These findings could pave the way for the discovery of promising modified structures and new candidates for treating inflammatory diseases and exhibiting anticancer activity.

Experimental

General

All chemicals were purchased from Merck, Fluka, Sigma-Aldrich and Acros chemical companies. These chemicals were used without more purification. CH_2Cl_2 and Et_3N were dried over CaH_2 by distillation before using. Infrared spectra and data were earned on a Shimadzu FT-IR 8300 spectrophotometer using potassium bromide pellets (ν in cm^{-1}). ^1H NMR and ^{13}C NMR spectra were obtained for samples dissolved in $CDCl_3$ or dimethylsulfoxide-d_6 (DMSO-d_6) using a Bruker Avance DPX instrument (^1H NMR at 250 MHz and 400 MHz; ^{13}C NMR at 100 MHz). Chemical shifts are expressed in parts per million (δ) downfield from tetramethylsilane. Coupling constants (J values) are expressed in hertz (Hz). Proton signal splitting patterns are determined as s: singlet, d: doublet, t: triplet, q: quartet, m: multiplet, dd: doublet of doublet. Melting points were measured on a Buchi 510 melting point device. Elemental analyses were done on a Thermo Finnigan Flash EA-1112 series instrument. Thin-layer chromatography (TLC) was done on silica gel 254 plates.

Procedure for the preparation of indole-3-acetic acid (2)

A mixture of indole-3-acetonitrile (1, 20 mmol, 3.12 g) in 25 ml of methanol and potassium hydroxide (162 mmol, 9.09 g) in 80 ml water was refluxed for about 3 h. The mixture was cooled in an ice-water bath and 6 N aqueous HCl solution was added to reach a pH = 1. The precipitate was filtered and washed with water then air-dried to give indole-3-acetic acid (2) [39].

General procedure for the preparation of Schiff bases 3a–o and 8a–l

A mixture of aryl aldehydes (5.00 mmol), aniline derivatives (5.00 mmol), and a few drops of glacial HOAc were mixed in 15 ml ethanol and this mixture was refluxed for an appropriate time 2−8 h (check by TLC). Then the mixture was cooled to room temperature, filtered and washed with cold ethanol to obtain the desired Schiff bases (3a−o and 8a−l).

Typical procedure for the synthesis of indolo-ß-lactam hybrid 4a

A mixture of indole-3-acetic acid (2, 1.5 mmol, 0.26 g), freshly-prepared Schiff base 3a (1 mmol, 0.26 g), *p*-toluenesulfonyl chloride (1.5 mmol, 0.28 g) and dry

Table 3 Anti-inflammatory activity and calculated free binding energies of compounds 4a–o and 9a–l

Cpd	$IC_{50\ NO\text{-}release}$ (μM)	$IC_{50\ cell\ viability}$ (μM)	Anti-inflammatory ratio	$\Delta G_{binding}$ (kcal/mol)[a]
4a	20.65 ± 1.98	>500	>24.21	−9.2
4b	8.10 ± 1.10	26.35 ± 1.35	3.25	−9.4
4c	0.88 ± 0.04	22.65 ± 1.76	25.74	−9.1
4d	2.85 ± 0.79	11.18 ± 0.89	3.92	−8.6
4e	0.62 ± 0.04	53.26 ± 3.57	85.90	−9.5
4f	1.04 ± 0.13	19.93 ± 1.94	19.16	−8.7
4g	1.32 ± 0.55	9.18 ± 1.05	6.95	−9.6
4h	>500	<500	–	−11.0
4i	>500	<500	–	−9.8
4j	1.97 ± 0.98	30.84 ± 2.34	15.65	−10.1
4k	22.99 ± 3.33	28.36 ± 2.28	1.23	−8.9
4l	1.92 ± 0.09	3.01 ± 0.93	1.57	−9.6
4m	12.54 ± 1.78	15.64 ± 1.84	1.25	−8.9
4n	<0.5	<1	–	−9.3
4o	<0.5	18.11 ± 2.05	>36.2	−9.1
9a	18.28 ± 2.06	>500	>27.35	−11.0
9b	24.62 ± 3.38	>500	>20.31	−9.4
9c	8.59 ± 1.98	28.53 ± 1.56	3.32	−10.4
9d	12.98 ± 1.22	38.89 ± 1.33	3.00	−10.3
9e	15.43 ± 1.86	291.61 ± 12.89	18.90	−11.3
9f	>500	>500	–	−9.4
9g	>500	>500	–	−9.0
9h	>500	>500	–	−9.6
9i	>500	>500	–	−10.2
9j	16.95 ± 2.49	241.59 ± 11.34	14.25	−11.8
9k	1.73 ± 0.65	244.33 ± 10.28	141.23	−9.1
9l	41.21 ± 3.29	>500	>12.13	−11.8
Dex.	4.31 ± 0.77	163.22 ± 9.34	37.87	−8.8

[a]Results has been calculated based on the interaction with the 4nos protein

triethylamine (5 mmol, 0.7 ml) in dry CH_2Cl_2 (10 ml) was stirred at room temperature for several hours. The reaction progress was monitored by thin layer chromatography (TLC) and the presence of a new compound was confirmed. Then the mixture was washed sequentially with 1 N aqueous HCl solution (10 ml), saturated aqueous $NaHCO_3$ solution (10 ml) and brine (10 ml). The organic layer was dried over solid Na_2SO_4, filtered and the solvent was evaporated to give a crude product that could be further purified by recrystallization from cold ethanol to give the purified indolo-β-lactam 4a in 80% yield.

3-(1H-Indol-3-yl)-1-(4-methoxyphenyl)-4-(2-nitrophenyl)azetidin-2-one (4a): Cream solid, 80%; mp 225–228 °C; IR (KBr) ν_{max} 3364 (N–H), 1743 (C=O),1512 (C–N indole), 1242 (Ar–O) cm^{-1}; ^1H NMR (250 MHz, $CDCl_3$) δ 8.11 (1H, broad, NH), 7.80 (1H, d, J = 7.5 Hz, ArH), 6.85–7.53 (12H, m, ArH), 6.21 (1H, d, J = 5.8 Hz, H-4), 5.45 (1H, d, J = 5.8 Hz, H-3), 3.80 (3H, s, O-CH_3); ^{13}C NMR (100 MHz, $CDCl_3$) δ 166.2 (C, CO), 156.2, 135.8, 133.3, 132.3, 131.3, 129.0, 128.4, 126.6, 125.3, 124.6, 122.1, 119.7, 119.0, 118.4, 114.6, 110.8, 105.9, 58.8 (CH, C-4), 55.5 (CH_3, O-CH_3), 53.6 (CH, C-3); Anal. Calcd. for $C_{24}H_{19}N_3O_4$: C, 69.72; H, 4.63; N, 10.16. Found: C, 69.22; H, 4.15; N, 10.10.

(3S,4S)-3-(1H-Indol-3-yl)-1-(4-methoxyphenyl)-4-(4-nitrophenyl)azetidin-2-one (4b): Yellowish small needles (EtOH); Pale yellow solid, 77%; mp 237–240 °C; IR (KBr) ν_{max} 3441 (N–H), 1736 (C=O), 1489 (N–H bending) cm^{-1}; ^1H NMR (400 MHz, DMSO-d_6) δ 10.90 (1H, s, NH), 7.89 (2H, d, J = 8.8 Hz, ArH), 7.47 (1H, d, J = 8.0 Hz, ArH), 7.42 (2H, d, J = 8.8 Hz, ArH), 7.30 (2H, d, J = 8.8 Hz, ArH), 7.18 (1H, d, J = 8.0 Hz, ArH), 7.16 (1H, d, J = 2.0 Hz, ArH), 6.88–6.99 (4H, m, ArH), 5.85 (1H, d, J = 6.0 Hz, H-4), 5.42 (1H, d, J = 6.0 Hz, H-3), 3.70 (3H, s, O-CH_3); ^{13}C NMR (100 MHz, DMSO-d_6) δ 165.4 (C, CO), 155.6, 146.5, 143.9, 135.7, 130.8, 128.4, 126.4, 124.5, 122.6, 121.2, 118.5, 118.2, 118.1, 114.5, 111.3, 105.1, 58.9 (CH, C-4), 55.2 (CH_3, O-CH_3), 52.6 (CH, C-3); Anal. Calcd. for $C_{24}H_{19}N_3O_4$: C, 69.72; H, 4.63; N, 10.16. Found: C, 69.31; H, 4.23; N, 10.12.

(1-(4-Bromophenyl)-3-(1H-indol-3-yl)-4-(2-nitrophenyl) azetidin-2-one (4c): Cream solid, 70%; mp 260–264 °C; IR (KBr) ν_{max} 3410 (N–H), 1743 (C=O), 1527 (C–N indole), 1489 (N–H bending) cm^{-1}; ^1H NMR (400 MHz, DMSO-d_6) δ 10.90 (1H, s, NH), 7.88 (1H, d, J = 7.6 Hz, ArH), 6.80–7.60 (12H, m, ArH), 6.26 (1H, d, J = 5.2 Hz, H-4), 5.55 (1H, d, J = 5.2 Hz, H-3); ^{13}C NMR (100 MHz, DMSO-d_6) δ 167.2 (C, CO), 147.0, 137.2, 135.5, 133.7, 132.1, 129.2, 126.5, 125.3, 125.1, 121.2, 119.1, 118.5, 115.6, 111.2, 104.5, 58.7 (CH, C-4), 53.2 (CH, C-3); Anal. Calcd. for $C_{23}H_{16}BrN_3O_3$: C, 59.76; H, 3.49; N, 9.09. Found: C, 58.88; H, 4.03; N, 9.18.

1-(2,4-Dimethoxyphenyl)-3-(1H-indol-3-yl)-4-(2-nitrophenyl)azetidin-2-one (4d): Pale green solid, 85%; mp 169–172 °C; IR (KBr) ν_{max} 3333 (N–H), 1728 (C=O), 1520 (C–N indole) cm^{-1}; ^1H NMR (250 MHz, $CDCl_3$) δ 8.50 (1H, broad, NH), 7.91 (1H, d, J = 8.8 Hz, ArH), 7.67 (1H, d, J = 8.3 Hz, ArH), 7.59 (1H, d, J = 6.8 Hz, ArH), 7.40 (1H, d, J = 7.8 Hz, ArH), 6.84–7.25 (6H, m, ArH), 6.53 (1H, dd, J = 2.5, 8.8 Hz, ArH), 6.45 (1H, d, J = 5.8 Hz, H-4), 6.42 (1H, d, J = 2.5 Hz, ArH), 5.39 (1H, d, J = 5.8 Hz, H-3), 3.78 (3H, s, O-CH_3), 3.58 (3H, s, O-CH_3); ^{13}C NMR (100 MHz, $CDCl_3$) δ 168.0 (C, CO), 158.5, 152.5, 147.4, 135.9, 133.9, 133.0, 128.3, 127.9, 126.6, 124.7, 121.8, 119.4, 119.0, 111.0, 106.5, 104.7, 99.8, 61.5 (CH, C-4), 55.6 (CH_3, O-CH_3), 55.5 (CH_3, O-CH_3), 54.0 (CH, C-3); Anal. Calcd. for $C_{25}H_{21}N_3O_5$: C, 67.71; H, 4.77; N, 9.48. Found: C, 68.85; H, 5.12; N, 9.31.

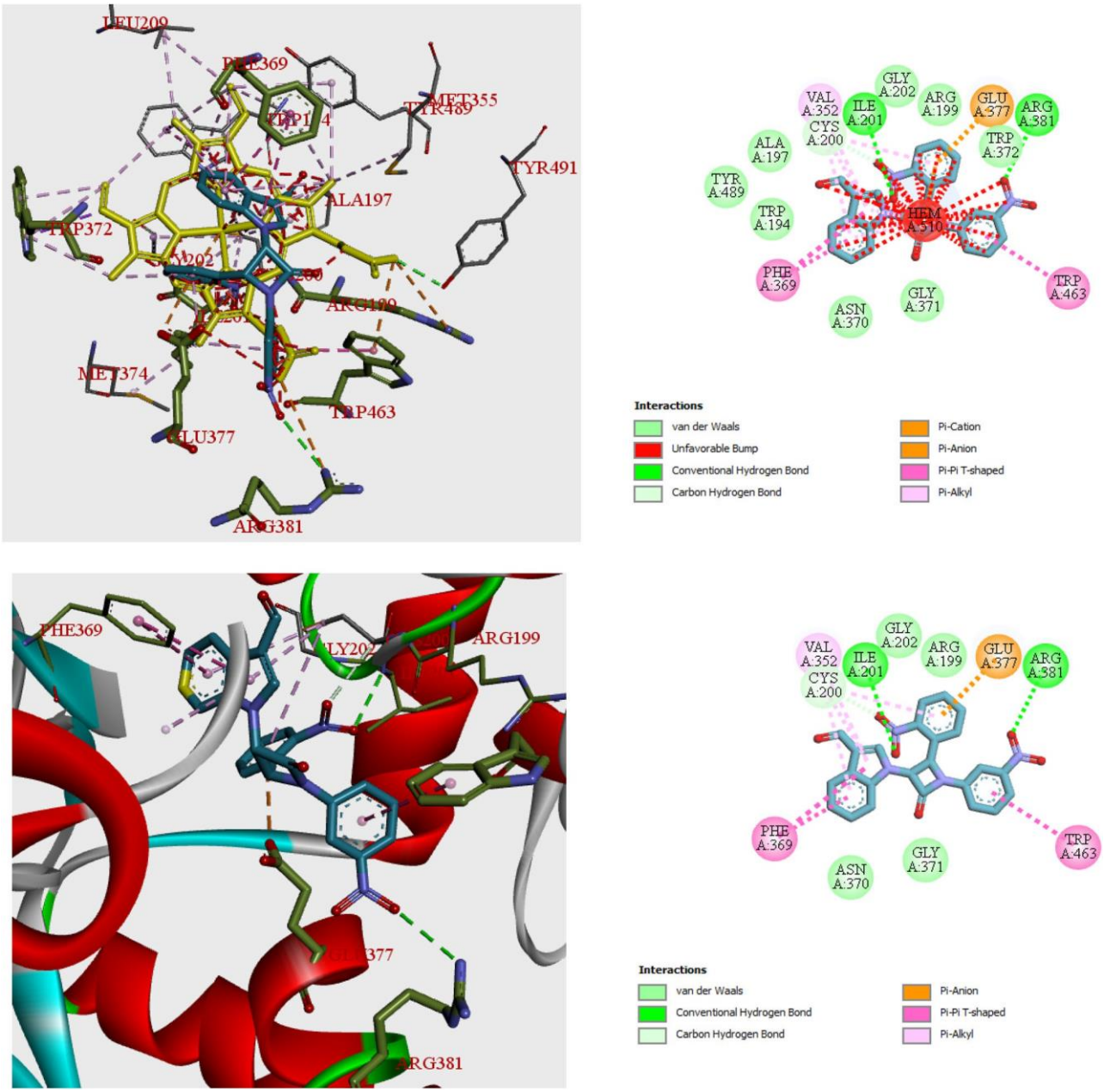

Fig. 6 The best pose of the most active compound 9k in the active site of human inducible nitric oxide synthase (PDB code: 4nos) and the residues of the active site involved in ligand binding; interactions with HEM and without HEM

3-(1H-indol-3-yl)-4-(2-nitrophenyl)-1-(3-nitrophenyl) azetidin-2-one (4e): Cream solid, 77%; mp 121−125 °C; IR (KBr) ν_{max} 3448 (N−H), 1759 (C=O), 1527 (C−N indole), 1350 (Ar−N) cm^{-1}; ^1H NMR (250 MHz, $CDCl_3$) δ 8.23 (2H, t, J = 2.0 Hz, ArH, NH), 8.01 (1H, dq, J = 1.0, 8.3 Hz, ArH), 7.83−7.90 (2H, m, ArH), 6.95−7.59 (8H, m, ArH), 6.89 (1H, d, J = 2.5 Hz, ArH), 6.37 (1H, d, J = 6.0 Hz, H-4), 5.55 (1H, d, J = 6.0 Hz, H-3); ^{13}C NMR (100 MHz, $CDCl_3$) δ 167.7 (C, CO), 148.8, 147.2, 138.7, 135.9, 133.7, 131.2, 130.4, 129.3, 128.4, 126.3, 125.6, 125.0, 122.7, 122.0, 119.7, 118.9, 118.7, 111.8, 111.3, 104.8, 59.4 (CH, C-4), 54.3 (CH, C-3); Anal. Calcd. for $C_{23}H_{16}N_4O_5$: C, 64.48; H, 3.76; N, 13.08. Found: C, 65.63; H, 4.16; N, 13.27.

4-(4-Bromophenyl)-3-(1H-indol-3-yl)-1-(4-methoxyphenyl)azetidin-2-one (4f): Cream solid, 76%; mp 239−243 °C; IR (KBr) ν_{max} 3394 (N−H), 1743 (C=O), 1512 (C−N indole), 1242 (Ar−O) cm^{-1}; ^1H NMR (400 MHz, DMSO-d_6) δ 10.90 (1H, s, NH), 7.45 (1H, d, J = 8.0 Hz, ArH), 7.20−7.29 (5H, m, ArH), 7.09 (3H, d, J = 8.0 Hz, ArH), 6.88−7.01 (4H, m, ArH), 5.67 (1H, d, J = 5.6 Hz, H-4), 5.31 (1H, d, J = 5.6 Hz, H-3), 3.70 (3H, s, O-CH_3); ^{13}C

NMR (100 MHz, DMSO-d_6) δ 165.6 (C, CO), 155.5, 135.7, 135.1, 130.9, 130.6, 129.0, 126.6, 124.4, 121.0, 120.0, 118.5, 118.3, 118.0, 114.5, 111.0, 105.0, 58.9 (CH, C-4), 55.0 (CH_3, O-CH_3), 52.2 (CH, C-3); Anal. Calcd. for $C_{24}H_{19}BrN_2O_2$: C, 64.44; H, 4.28; N, 6.26. Found: C, 65.51; H, 4.78; N, 5.83.

4-(4-Chlorophenyl)-3-(1H-indol-3-yl)-1-(4-methoxyphenyl)azetidin-2-one (4g): Cream solid, 75%; mp 244−247 °C; IR (KBr) ν_{max} 3394 (N−H), 1743 (C=O), 1512 (C−N indole), 1242 (Ar−O) cm^{-1}; ^{1}H NMR (400 MHz, DMSO-d_6) 10.90 (1H, s, NH), 6.88−7.53 (20H, m, ArH), 5.69 (1H, d, J = 5.6 Hz, H-4), 5.32 (1H, d, J = 5.6 Hz, H-3), 3.70 (3H, s, O-CH_3); ^{13}C NMR (100 MHz, DMSO-d_6) δ 165.7 (C, CO), 155.5, 135.7, 134.7, 131.8, 130.9, 129.0, 128.9, 128.3, 127.7, 126.6, 124.4, 121.1, 118.4, 118.3, 118.1 , 114.5, 114.4, 111.2, 105.5, 58.8 (CH, C-4), 55.0 (CH_3, O-CH_3), 52.2 (CH, C-3); Anal. Calcd. for $C_{24}H_{19}ClN_2O_2$: C, 71.55; H, 4.75; N, 6.95. Found: C, 72.46; H, 5.22; N, 6.52.

4-(Anthracen-9-yl)-3-(1H-indol-3-yl)-1-(4-methoxyphenyl)azetidin-2-one (4h): Pale yellow solid, 87%; mp 205−208 °C; IR (KBr) ν_{max} 3394 (N−H), 1751 (C=O), 1520 (C−N indole), 1489 (N−H bending) cm^{-1}; ^{1}H NMR (400 MHz, DMSO-d_6) δ 10.63 (1H, s, NH), 8.78 (1H, d, J = 8.8 Hz, ArH), 8.72 (1H, t, J = 2.8 Hz, ArH), 8.40 (1H, s, ArH), 7.98 (1H, d, J = 8.4 Hz, ArH), 7.87 (1H, t, J = 6.4 Hz, ArH), 7.67 (1H, t, J = 7.2 Hz, ArH), 7.51 (1H, t, J = 7.2 Hz, ArH), 7.40 (1H, d, J = 7.6 Hz, ArH), 7.27−7.30 (2H, m, ArH), 7.18 (2H, d, J = 8.0 Hz, ArH), 6.95−7.03 (3H, m, ArH), 6.80 (3H, m, H-4, ArH), 6.67 (1H, t, J = 7.2 Hz, ArH), 5.88 (1H, d, J = 6.0 Hz, H-3), 3.62 (3H, s, O-CH_3); ^{13}C NMR (100 MHz, DMSO-d_6) δ 166.3 (C, CO), 155.5, 135.1, 131.9, 130.9, 130.5, 130.3, 129.8, 129.1, 129.0, 128.5, 126.9, 126.5, 125.5, 125.2, 125.1, 124.7, 124.5, 124.3, 123.6, 120.8, 118.2, 118.0, 117.5, 114.5, 111.2, 105.0, 59.2 (CH, C-4), 55.2 (CH_3, O-CH_3), 53.0 (CH, C-3); Anal. Calcd. for $C_{32}H_{24}N_2O_2$: C, 82.03; H, 5.16; N, 5.98. Found: C, 79.94; H, 4.61; N, 6.57.

1-(2,3-Dihydrobenzo[b][1,4]dioxin-6-yl)-3-(1H-indol-3-yl)-4-(2-nitrophenyl)azetidin-2-one (4i): Pale green solid, 78%; mp 220−223 °C; IR (KBr) ν_{max} 3340 (N−H), 1728 (C=O), 1512 (C−N indole) cm^{-1}; ^{1}H NMR (400 MHz, DMSO-d_6) δ 10.87 (1H, s, NH), 7.86 (1H, d, J = 8.0 Hz, ArH), 7.53 (1H, t, J = 7.2 Hz, ArH), 7.44 (2H, t, J = 7.2 Hz, ArH), 7.31 (1H, t, J = 8.0 Hz, ArH), 7.16 (1H, d, J = 8.0 Hz, ArH), 7.04 (1H, d, J = 2.4 Hz, ArH), 6.86−6.97 (5H, m, ArH), 6.19 (1H, d, J = 6.0 Hz, H-4), 5.48 (1H, d, J = 6.0 Hz, H-3), 4.23 (4H, s, O-C$\underline{H}_2$C$\underline{H}_2$-O); ^{13}C NMR (100 MHz, DMSO-d_6) δ 166.6 (C, CO), 147.2, 143.5, 139.9, 135.5, 133.6, 132.3,, 131.4, 128.8, 128.5, 126.6, 125.2, 124.8, 120.9, 118.5, 117.4, 111.2, 110.3, 106.2, 104.8, 64.2 (CH_2, O-$\underline{C}H_2CH_2$-O), 63.9 (CH_2, O-$CH_2\underline{C}H_2$-O), 58.5 (CH, C-4), 52.9 (CH, C-3); Anal. Calcd. for $C_{25}H_{19}N_3O_5$: C, 68.02; H, 4.34; N, 9.52. Found: C, 68.74; H, 4.86; N, 9.37.

1-(4-Ethoxyphenyl)-3-(1H-indol-3-yl)-4-(2-nitrophenyl) azetidin-2-one (4j): Orange solid, 93%; mp 206−210 °C; IR (KBr) ν_{max} 3340 (N−H), 1743 (C=O), 1512 (C−N indole) cm^{-1}; ^{1}H NMR (250 MHz, $CDCl_3$) δ 8.43 (1H, broad, NH), 7.79 (1H, dd, J = 1.0, 8.0 Hz, ArH), 6.84−7.51 (11H, m, ArH), 6.78 (1H, d, J = 2.5 Hz, ArH), 6.19 (1H, d, J = 5.8 Hz, H-4), 5.41 (1H, d, J = 5.8 Hz, H-3), 4.01 (2H, q, J = 7.0 Hz, O-C$\underline{H}_2$CH$_3$), 1.40 (3H, t, J = 7.0 Hz, O-CH$_2$C$\underline{H}_3$); ^{13}C NMR (100 MHz, $CDCl_3$) δ 166.7 (C, CO), 155.7, 147.2, 135.8, 133.4, 132.3, 131.2, 129.0, 128.5, 126.5, 125.3, 124.8, 121.9, 119.6, 118.9, 118.4, 115.3, 111.2, 105.7, 63.8 (CH_2, O-$\underline{C}H_2CH_3$), 58.9 (CH, C-4), 53.5 (CH, C-3), 14.8 (CH_3, O-$CH_2\underline{C}H_3$); Anal. Calcd. for $C_{25}H_{21}N_3O_4$: C, 70.25; H, 4.95; N, 9.83. Found: C, 69.93; H, 5.39; N, 9.78.

1-(4-Ethoxyphenyl)-3-(1H-indol-3-yl)-4-(m-tolyl)azetidin-2-one (4k): Cream solid, 84%; mp 171−174 °C; IR (KBr) ν_{max} 3271 (N−H), 1728 (C=O), 1512 (C−N indole) cm^{-1}; ^{1}H NMR (250 MHz, $CDCl_3$) δ 7.95 (1H, broad, NH), 7.38 (1H, t, J = 3.3 Hz, ArH), 7.34 (1H, t, J = 3.3 Hz, ArH), 7.26 (1H, s, ArH), 7.17 (1H, d, J = 7.5 Hz, ArH), 7.07 (1H, dd, J = 1.3, 7.0 Hz, ArH), 7.03 (1H, t, J = 1.8 Hz, ArH), 6.75−7.01 (6H, m, ArH), 5.44 (1H, d, J = 5.8 Hz, H-4), 5.20 (1H, d, J = 5.8 Hz, H-3), 3.97 (2H, q, J = 7.0 Hz, O-C$\underline{H}_2$CH$_3$), 2.06 (3H, s, CH_3), 1.38 (3H, t, J = 7.0 Hz, O-CH$_2$C$\underline{H}_3$); ^{13}C NMR (100 MHz, $CDCl_3$) δ 166.0 (C, CO), 155.4, 137.4, 135.8, 134.9, 131.5, 128.4, 127.9, 127.7, 126.9, 124.0, 123.5, 121.9, 119.2, 118.6, 118.5, 114.9, 110.9, 107.1, 63.7 (CH_2, O-$\underline{C}H_2CH_3$), 60.4 (CH, C-4), 52.7 (CH, C-3), 21.2 (CH_3), 14.8 (CH_3, O-$CH_2\underline{C}H_3$); Anal. Calcd. for $C_{26}H_{24}N_2O_2$: C, 78.76; H, 6.10; N, 7.07. Found: C, 76.87; H, 7.33; N, 7.85.

4-(4-Chlorophenyl)-1-(4-ethoxyphenyl)-3-(1H-indol-3-yl)azetidin-2-one (4l): Cream solid, 74%; mp 162−165 °C; IR (KBr) ν_{max} 3401 (N−H), 1728 (C=O), 1512 (C−N indole), 1234 (Ar−O) cm^{-1}; ^{1}H NMR (400 MHz, DMSO-d_6) δ 11.20 (1H, s, NH), 6.88−7.53 (13H, m, ArH), 5.68 (1H, d, J = 5.6 Hz, H-4), 5.32 (1H, d, J = 5.6 Hz, H-3), 3.96 (2H, q, J = 6.8 Hz, O-C$\underline{H}_2$CH$_3$), 1.29 (3H, t, J = 6.8 Hz, O-CH$_2$C$\underline{H}_3$); ^{13}C NMR (100 MHz, DMSO-d_6) δ 165.5 (C, CO), 154.9, 137.0, 136.5, 135.7, 132.8, 131.8, 130.5, 128.9, 128.3, 127.7, 125.8, 124.2, 121.5, 119.0, 118.2 , 118.0, 114.9, 111.9, 111.3, 107.5, 63.0 (CH_2, O-$\underline{C}H_2CH_3$), 60.7 (CH, C-4), 57.6 (CH, C-3), 14.6 (CH_3, O-$CH_2\underline{C}H_3$); Anal. Calcd. for $C_{25}H_{21}ClN_2O_2$: C, 72.02; H, 5.08; N, 6.72. Found: C, 73.35; H, 5.45; N, 6.25.

4-(3,4-Dimethoxyphenyl)-1-(4-ethoxyphenyl)-3-(1H-indol-3-yl)azetidin-2-one (4m): Cream solid, 76%; mp 182−185 °C; IR (KBr) ν_{max} 3364 (N−H), 1736 (C=O), 1512 (C−N indole), 1234 (Ar−O) cm^{-1}; ^{1}H NMR (250 MHz, $CDCl_3$) δ 8.07 (1H, broad, NH), 7.46 (1H, d, J = 7.8 Hz,

ArH), 7.37 (2H, d, J = 9.0 Hz, ArH), 7.18 (1H, d, J = 7.8 Hz, ArH), 7.07 (1H, t, J = 7.2 Hz, ArH), 6.99 (2H, t, J = 7.2 Hz, ArH), 6.82 (2H, d, J = 9.0 Hz, ArH), 6.70 (1H, d, J = 8.1 Hz, ArH), 6.52 (2H, t, J = 4.5 Hz, ArH), 5.42 (1H, d, J = 5.7 Hz, H-4), 5.19 (1H, d, J = 5.7 Hz, H-3), 3.98 (2H, q, J = 6.9 Hz, O-C$\underline{H}_2$CH$_3$), 3.68 (3H, s, O-CH$_3$), 3.44 (3H, s, O-CH$_3$), 1.38 (3H, t, J = 6.9 Hz, O-CH$_2$C$\underline{H}_3$); ^{13}C NMR (100 MHz, $CDCl_3$) δ 166.0 (C, CO), 155.4, 148.4, 148.3, 135.9, 131.5, 127.5, 126.9, 123.4, 122.2, 119.7, 119.4, 118.5, 114.9, 111.2, 110.3, 110.1, 107.3, 63.4 (CH$_2$, O-$\underline{C}$H$_2$CH$_3$), 60.2 (CH, C-4), 55.6 (CH$_3$, O-CH$_3$, O-CH$_3$), 52.7 (CH, C-3), 14.8 (CH$_3$, O-CH$_2\underline{C}$H$_3$); Anal. Calcd. for $C_{27}H_{26}N_2O_4$: C, 73.28; H, 5.92; N, 6.33. Found: C, 74.50; H, 6.24; N, 6.12.

1-(4-Ethoxyphenyl)-3-(1H-indol-3-yl)-4-(3-nitrophenyl) azetidin-2-one (4n): Red solid, 86%; mp 118−121 °C; IR (KBr) ν_{max} 3402 (N−H), 1728 (C=O), 1520 (C−N indole), 1342 (Ar−N) cm^{-1}; ^{1}H NMR (250 MHz, $CDCl_3$) δ 8.22 (1H, broad, NH), 7.82 (2H, d, J = 9.0 Hz, ArH), 7.38 (1H, d, J = 7.8, ArH), 6.90−7.30 (8H, m, ArH), 6.66 (2H, d, J = 9.0 Hz, ArH), 5.55 (1H, d, J = 5.5 Hz, H-4), 5.28 (1H, d, J = 5.5 Hz, H-3), 3.71 (2H, q, J = 7.0 Hz, O-C$\underline{H}_2$CH$_3$), 1.24 (3H, t, J = 7.0 Hz, O-CH$_2$C$\underline{H}_3$); ^{13}C NMR (100 MHz, $CDCl_3$) δ 164.7 (C, CO), 147.8, 147.2, 143.3, 135.9, 127.9, 127.6, 126.3, 123.8, 123.0, 122.3, 119.5, 118.3, 118.1, 113.1, 111.4, 106.4, 59.6 (CH$_2$, O-$\underline{C}$H$_2$CH$_3$), 58.4 (CH, C-4), 52.9 (CH, C-3), 18.4 (CH$_3$, O-CH$_2\underline{C}$H$_3$); Anal. Calcd. for $C_{25}H_{21}N_3O_4$: C, 70.25; H, 4.95; N, 9.83. Found: C, 71.75; H, 5.36; N, 9.44.

3-(1H-Indol-3-yl)-1-(4-iodophenyl)-4-(2-nitrophenyl) azetidin-2-one (4o): Pale yellow solid, 73%; mp >260 °C; IR (KBr) ν_{max} 3326 (N−H), 1743 (C=O), 1520 (C−N indole), 1481 (N−H bending) cm^{-1}; ^{1}H NMR (400 MHz, DMSO-d_6) δ 10.86 (1H, s, NH), 7.84 (1H, d, J = 7.6 Hz, ArH), 7.68 (2H, d, J = 8.4 Hz, ArH), 7.49 (1H, t, J = 6.8 Hz, ArH), 7.39 (2H, t, J = 9.2 Hz, ArH), 7.16−7.32 (3H, m, ArH), 7.12 (1H, d, J = 8.0 Hz, ArH), 6.76−6.96 (3H, m, ArH), 6.22 (1H, d, J = 6.0 Hz, H-4), 5.49 (1H, d, J = 6.0 Hz, H-3); ^{13}C NMR (100 MHz, DMSO-d_6) δ 167.3 (C, CO), 147.0, 137.8, 137.2, 135.5, 133.7, 132.0, 128.8, 128.7, 126.5, 125.3, 124.9, 120.9, 119.3, 118.5, 118.4, 111.2, 104.5, 58.6 (CH, C-4), 53.2 (CH, C-3); Anal. Calcd. for $C_{23}H_{16}IN_3O_3$: C, 54.24; H, 3.17; N, 8.25. Found: C, 55.65; H, 3.85; N, 8.02.

Procedure for preparation of indole-3-carbaldehyde (6)

Dimethylformamide (14.5 ml) was added to a flask cooled in an ice-salt for 30 min. Phosphoryl trichloride (4.4 ml) was added dropwise with stirring over 20 min. To this was added dropwise over 30 min a solution of 4.95 g of indole (5) in 10 ml of dimethylformamide. The temperature was not allowed to rise above 10 °C during this time. Then mixture was stirred at room temperature for about 2−3 h. The temperature of mixture was raised to 35 °C and stirred at this temperature for 30 min. Crushed ice was added to the mixture and 35 ml of 15% sodium hydroxide solution was added dropwise with careful stirring. The 65 ml of remaining sodium hydroxide solution was added more quickly with efficient stirring. The canary-yellow paste was observed at this time. The resulting suspension was heated quickly to the boiling point and stirred in this temperature for 5 min. Then the mixture was allowed to cool in an ice bath for 1 h. The produced precipitate was filtered and resuspended in water to remove DMF and soluble inorganic material. Product was collected on a filter and air-dried. The indole-3-carbaldehyde (6) was obtained with an efficiency of 80%, without the need for more purification.

Procedure for preparation of *N*-acetic acid indole-3-carbaldehyde (7)

A mixture of indole-3-carbaldehyde (6) (10 mmol, 1.45 g) and calcium hydride (15 mmol, 0.63 g) in 5 ml of dry dimethylformamide was stirred for 30 min. Then bromoacetic acid (15 mmol, 2.08 g) was added and stirred at room temperature overnight. For workup, water 25 ml and ethyl acetate 25 ml was added and organic phase was separated to remove unreacted indole-3-carbaldehyde. Then a 2 N aqueous HCl solution was added to the aqueous layer to acidify the pH and was extracted with 25 ml of ethyl acetate. The organic layer was dried over solid Na_2SO_4 and the solvent was evaporated to give *N*-acetic acid indole-3-carbaldehyde (7) in 70% yield.

Typical procedure for synthesis of new indole-3-carbaldehyde β-lactam hybrids 9a-l

A mixture of *N*-acetic acid indole-3-carbaldehyde (7, 1.0 mmol, 0.203 g), Schiff base 8a (0.3 mmol, 0.08 g), *p*-toluenesulfonyl chloride (1.0 mmol, 0.18 g) and dry triethylamine (4 mmol, 0.55 ml) in dry CH_2Cl_2 (7 ml) was stirred at room temperature for an appropriate time. Thin layer chromatography (TLC) was used for monitoring reaction progress. At the end of the reaction, the mixture was washed sequentially with 1 N aqueous HCl solution (10 ml), aqueous saturated $NaHCO_3$ solution (10 ml) and brine (10 ml), respectively. The organic layer was dried over solid Na_2SO_4, filtered and the solvent was evaporated to give a crude product that was purified by ethanol to give purified indole-3-carbaldehyde β-lactam 9a in 78% yield.

1-(1-(4-ethoxyphenyl)-2-(3-nitrophenyl)-4-oxoazetidin-3-yl)-1H-indole-3-carbaldehyde (9a): Brown solid, 78%; mp 180−183 °C; IR (KBr) ν_{max} 1748 (C=O), 1658 (HC=O), 1520 (C−N indole), 1350 (Ar−N) cm^{-1}; ^{1}H NMR (400 MHz, $CDCl_3$) δ 9.88 (1H, s, CHO), 8.14 (2H, d, J = 8.0 Hz, ArH), 7.88 (2H, d, J = 8.8 Hz, ArH), 7.80 (1H,

s, ArH), 7.25−7.33 (7H, m, ArH), 6.68 (2H, d, J = 9.2 Hz, ArH), 6.17 (1H, d, J = 5.2 Hz, H-4), 5.71 (1H, d, J = 5.2 Hz, H-3), 3.95 (2H, q, J = 6.8 Hz, O-C<u>H</u>$_2$CH$_3$), 1.60 (3H, t, J = 6.8 Hz, O-CH$_2$C<u>H</u>$_3$); ^{13}C NMR (100 MHz, CDCl$_3$) δ 185.4 (CHO), 158.1 (CO), 156.8, 148.3, 139.3, 136.5, 129.6, 127.5, 125.8, 125.0, 124.4, 123.7, 122.0, 119.0, 118.0, 113.0, 109.0, 65.1 (CH, C-3), 60.7 (CH$_2$, O-<u>C</u>H$_2$CH$_3$), 58.0 (CH, C-4), 18.0 (CH$_3$, O-CH$_2$<u>C</u>H$_3$); Anal. Calcd. for $C_{26}H_{21}N_3O_5$: C, 68.56; H, 4.65; N, 9.23. Found: C, 67.22; H, 4.15; N, 10.1.

1-(2-(anthracen-9-yl)-1-(4-methoxyphenyl)-4-oxoazetidin-3-yl)-1H-indole-3-carbaldehyde (9b): Brown solid, 75%; mp 224−227 °C; IR (KBr) ν_{max} 1751 (C=O), 1658 (HC=O), 1512 (C−N indole) cm^{-1}; ^{1}H NMR (400 MHz, CDCl$_3$) δ 9.37 (1H, s, CHO), 8.35 (1H, d, J = 8.8 Hz, ArH), 8.36 (1H, d, J = 9.2 Hz, ArH), 8.10 (1H, s, ArH), 7.64−7.76 (4H, m, ArH), 7.50 (1H, t, J = 7.6 Hz, ArH), 7.37 (2H, d, J = 8.8 Hz, ArH), 7.18−7.34 (4H, m, ArH), 6.97 (1H, d, J = 5.2 Hz, H-4), 6.71−6.90 (5H, m, ArH), 6.35 (1H, d, J = 5.2 Hz, H-3), 3.66 (3H, s, O-CH$_3$); ^{13}C NMR (100 MHz, CDCl$_3$) δ 184.4 (CHO), 160.2 (CO), 157.2, 138.6, 136.6, 131.3, 131.1, 130.7, 130.6, 130.1, 129.9, 127.3, 127.2, 124.8, 124.7, 124.1, 123.5, 123.3, 122.8, 121.7, 119.7, 118.7, 118.4, 114.8, 109.3, 66.0 (CH, C-3), 60.1 (CH, C-4), 55.0 (CH$_3$, O-CH$_3$); Anal. Calcd. for $C_{33}H_{24}N_2O_3$: C, 79.8; H, 4.87; N, 5.64. Found: C, 78.31; H, 4.23; N, 5.12.

1-((2S,3R)-1-(4-ethoxyphenyl)-2-(2-nitrophenyl)-4-oxoazetidin-3-yl)-1H-indole-3-carbaldehyde (9c): Yellowish small needles (EtOH); Pale yellow solid, 72%; mp 182−185 °C; IR (KBr) ν_{max} 1759 (C=O), 1666 (HC=O), 1512 (C−N indole) cm^{-1}; ^{1}H NMR (400 MHz, CDCl$_3$) δ 9.76 (1H, s, CHO), 8.10 (1H, d, J = 7.6 Hz, ArH), 7.90 (1H, d, J = 8.0 Hz, ArH), 7.22−7.60 (12H, m, ArH), 6.90 (2H, d, J = 8.8 Hz, ArH), 6.43 (1H, d, J = 5.2 Hz, H-4), 6.40 (1H, d, J = 5.2 Hz, H-3), 4.05 (2H, q, J = 6.8 Hz, O-C<u>H</u>$_2$CH$_3$), 1.44 (3H, t, J = 6.8 Hz, O-CH$_2$C<u>H</u>$_3$); ^{13}C NMR (100 MHz, CDCl$_3$) δ 184.6 (CHO), 160.3 (CO), 156.6, 147.1, 136.8, 134.2, 130.2, 129.8, 129.0, 126.1, 124.7, 124.6, 123.5, 121.9, 119.3, 118.8, 115.4, 110.3, 66.1 (CH, C-3), 64.0 (CH$_2$, O-<u>C</u>H$_2$CH$_3$), 60.0 (CH, C-4), 14.8 (CH$_3$, O-CH$_2$<u>C</u>H$_3$); Anal. Calcd. for $C_{26}H_{21}N_3O_5$: C, 68.56; H, 4.65; N, 9.23. Found: C, 69.23; H, 4.32; N, 9.02.

1-(1-(2,3-dihydrobenzo[b][1,4]dioxin-6-yl)-2-(2-nitrophenyl)-4-oxoazetidin-3-yl)-1H-indole-3-carbaldehyde (9d): Brown solid, 68%; mp 172−175 °C; IR (KBr) ν_{max} 1757 (C=O), 1656 (HC=O), 1527 (C−N indole) cm^{-1}; ^{1}H NMR (400 MHz, DMSO-d_6) δ 9.70 (1H, s, CHO), 8.10 (1H, s, ArH), 7.90 (2H, d, J = 8.8 Hz, ArH), 7.10−7.70 (8H, m, ArH), 6.96 (1H, d, J = 5.6 Hz, H-4), 6.92 (1H, d, J = 8.0 Hz, ArH), 6.40 (1H, d, J = 5.2 Hz, H-3), 4.25 (4H, s, O-C<u>H</u>$_2$C<u>H</u>$_2$-O); ^{13}C NMR (100 MHz, DMSO-d_6) δ 185.2 (CHO), 161.3 (CO), 147.2, 143.4, 140.7, 139.7, 137.1, 134.0, 129.7, 128.9, 125.1, 123.9, 123.5, 122.8, 120.7, 118.1, 117.5, 111.5, 110.9, 106.7, 65.6 (CH, C-3), 64.2 (CH$_2$, O-<u>C</u>H$_2$CH$_2$-O), 63.9 (CH$_2$, O-CH$_2$<u>C</u>H$_2$-O), 60.5 (CH, C-4); Anal. Calcd. for $C_{26}H_{19}N_3O_6$: C, 66.5; H, 4.08; N, 8.95. Found: C, 65.85; H, 4.56; N, 9.31.

1-(1-(4-methoxyphenyl)-2-(4-nitrophenyl)-4-oxoazetidin-3-yl)-1H-indole-3-carbaldehyde (9e): Cream solid, 68%; mp 193−196 °C; IR (KBr) ν_{max} 1759 (C=O), 1658 (HC=O), 1520 (C−N indole) cm^{-1}; ^{1}H NMR (400 MHz, CDCl$_3$) δ 9.78 (1H, s, CHO), 8.05 (1H, d, J = 7.6 Hz, ArH), 7.80 (2H, d, J = 8.8 Hz, ArH), 7.72 (1H, s, ArH), 7.15−7.27 (7H, m, ArH), 6.80 (2H, d, J = 8.8 Hz, ArH), 6.10 (1H, d, J = 5.2 Hz, H-4), 5.60 (1H, d, J = 5.2 Hz, H-3), 3.72 (3H, s, O-CH$_3$); ^{13}C NMR (100 MHz, CDCl$_3$) δ 184.6 (CHO), 158.7 (CO), 157.4, 148.1, 138.8, 136.3, 129.5, 127.6, 124.8, 124.6, 123.7, 123.6, 122.5, 119.2, 118.8, 114.6, 109.0, 65.2 (CH, C-3), 60.7 (CH, C-4), 55.5 (CH$_3$, O-CH$_3$); Anal. Calcd. for $C_{25}H_{19}N_3O_5$: C, 68.02; H, 4.34; N, 9.52. Found: C, 66.63; H, 4.16; N, 10.17.

1-((2R,3R)-1-(2,4-dimethoxyphenyl)-2-(2-nitrophenyl)-4-oxoazetidin-3-yl)-1H-indole-3-carbaldehyde (9f): Yellowish small cubics (EtOH); Pale yellow solid, 65%; mp 175−178 °C; IR (KBr) ν_{max} 1751 (C=O), 1666 (HC=O), 1520 (C−N indole) cm^{-1}; ^{1}H NMR (400 MHz, CDCl$_3$) δ 9.80 (1H, s, CHO), 8.10 (1H, d, J = 7.6 Hz, ArH), 8.01 (1H, d, J = 8.8 Hz, ArH), 7.81 (1H, d, J = 7.2 Hz, ArH), 7.21−7.62 (7H, m, ArH), 6.70 (1H, d, J = 5.2 Hz, H-4), 6.59 (1H, dd, J = 2.8, 8.8 Hz, ArH), 6.47 (1H, d, J = 2.8 Hz, ArH), 6.38 (1H, d, J = 5.2 Hz, H-3), 3.84 (3H, s, O-CH$_3$), 3.64 (3H, s, O-CH$_3$); ^{13}C NMR (100 MHz, CDCl$_3$) δ 184.8 (CHO), 161.9 (CO), 159.2, 152.2, 147.2, 137.1, 137.0, 133.7, 130.7, 129.5, 128.1, 125.6, 124.7, 124.5, 124.3, 123.3, 121.7, 119.1, 118.0, 110.5, 105.0, 100.1, 67.1 (CH, C-3), 63.0 (CH, C-4), 55.7 (CH$_3$, O-CH$_3$, O-CH$_3$); Anal. Calcd. for $C_{26}H_{21}N_3O_6$: C, 66.24; H, 4.49; N, 5.91. Found: C, 67.51; H, 4.68; N, 5.83.

1-(1-(4-methoxyphenyl)-2-(3-nitrophenyl)-4-oxoazetidin-3-yl)-1H-indole-3-carbaldehyde (9g): Cream solid, 76%; mp 232−235 °C; IR (KBr) ν_{max} 1757 (C=O), 1655 (HC=O), 1520 (C−N indole) cm^{-1}; ^{1}H NMR (400 MHz, CDCl$_3$) δ 9.80 (1H, s, CHO), 8.11 (1H, d, J = 7.6 Hz, ArH), 7.87 (2H, d, J = 8.4 Hz, ArH), 7.80 (1H, s, ArH), 7.23−7.34 (9H, m, ArH), 6.88 (2H, d, J = 8.8 Hz, ArH), 6.18 (1H, d, J = 5.2 Hz, H-4), 5.72 (1H, d, J = 5.2 Hz, H-3), 3.80 (3H, s, O-CH$_3$); ^{13}C NMR (100 MHz, CDCl$_3$) δ 184.2 (CHO), 158.6 (CO), 157.4, 148.1, 138.8, 136.3, 129.4, 127.6, 124.8, 124.4, 123.8, 123.6, 122.6, 119.2, 118.7, 114.8, 108.9, 64.7 (CH, C-3), 60.7 (CH, C-4), 55.0 (CH$_3$, O-CH$_3$); Anal. Calcd. for $C_{25}H_{19}N_3O_5$: C, 68.02; H, 4.34; N, 9.52. Found: C, 69.46; H, 4.82; N, 8.92.

4-(3-(3-formyl-1H-indol-1-yl)-1-(4-methoxyphenyl)-4-oxoazetidin-2-yl)benzonitrile (9h): Brown solid, 70%; mp 188−190 °C; IR (KBr) ν_{max} 1747 (C=O), 1659 (HC=O),

1520 (C−N indole) cm^{-1}; ^1H NMR (400 MHz, $CDCl_3$) δ 9.87 (1H, s, CHO), 8.14 (1H, d, J = 7.6 Hz, ArH), 7.79 (1H, s, ArH), 7.20−7.35 (9H, m, ArH), 6.89 (2H, d, J = 8.8 Hz, ArH), 6.16 (1H, d, J = 5.2 Hz, H-4), 5.67 (1H, d, J = 5.2 Hz, H-3), 3.81 (3H, s, O-CH_3); ^{13}C NMR (100 MHz, $CDCl_3$) δ 184.5 (CHO), 158.9 (CO), 157.2, 136.9, 136.4, 132.2, 129.6, 127.3, 124.9, 124.4, 123.7, 122.4, 119.1, 118.8, 117.6, 114.8, 112.9, 109.1, 65.2 (CH, C-3), 60.9 (CH, C-4), 55.5 (CH_3, O-CH_3); Anal. Calcd. for $C_{26}H_{19}N_3O_3$: C, 74.10; H, 4.54; N, 9.97. Found: C, 75.64; H, 4.01; N, 10.47.

1-(2-(anthracen-9-yl)-1-(4-(dimethylamino)phenyl)-4-oxoazetidin-3-yl)-1H-indole-3-carbaldehyde (9i): Yellow solid, 78%; mp 247−250 °C; IR (KBr) ν_{max} 1747 (C=O), 1657 (HC=O), 1520 (C−N indole) cm^{-1}; ^1H NMR (400 MHz, $CDCl_3$) δ 9.43 (1H, s, CHO), 8.65 (1H, d, J = 9.2 Hz, ArH), 8.43 (1H, d, J = 8.8 Hz, ArH), 8.16 (1H, s, ArH), 7.73−7.82 (4H, m, ArH), 7.58 (1H, t, J = 8.0 Hz, ArH), 7.26−7.41 (7H, m, ArH), 7.02 (1H, d, J = 5.2 Hz, H-4), 6.78−6.96 (3H, m, ArH), 6.58 (2H, d, J = 8.4 Hz, ArH), 6.39 (1H, d, J = 5.2 Hz, H-3), 2.88 (6H, s, $N(CH_3)_2$); ^{13}C NMR (100 MHz, $CDCl_3$) δ 184.5 (CHO), 159.4 (CO), 148.3, 138.8, 136.6, 131.2, 130.6, 130.3, 130.0, 129.8, 127.6, 127.2, 127.0, 124.7, 124.0, 123.5, 123.4, 122.7, 121.7, 121.6, 120.2, 118.7, 118.2, 112.8, 109.3, 65.9 (CH, C-3), 60.5 (CH, C-4), 40.5 (CH_3, $N(CH_3)_2$); Anal. Calcd. for $C_{34}H_{27}N_3O_2$: C, 80.13; H, 5.34; N, 8.25. Found: C, 78.74; H, 5.16; N, 8.57.

1-(2-(anthracen-9-yl)-4-oxo-1-phenylazetidin-3-yl)-1H-indole-3-carbaldehyde (9j): Pale yellow solid, 68%; mp >250 °C; IR (KBr) ν_{max} 1761 (C=O), 1660 (HC=O), 1541 (C−N indole) cm^{-1}; ^1H NMR (400 MHz, $CDCl_3$) δ 9.44 (1H, s, CHO), 8.62 (1H, d, J = 9.2 Hz, ArH), 8.44 (1H, d, J = 9.2 Hz, ArH), 8.18 (1H, s, ArH), 7.81 (2H, t, J = 7.2 Hz, ArH), 7.75 (1H, d, J = 8.0 Hz, ArH), 7.70 (1H, s, ArH), 7.60 (1H, t, J = 8.0 Hz, ArH), 7.51 (2H, d, J = 8.0 Hz, ArH), 7.39 (1H, t, J = 7.6 Hz, ArH), 7.26−7.35 (5H, m, ArH), 7.15 (1H, t, J = 7.2 Hz, ArH), 7.10 (1H, d, J = 5.2 Hz, H-4), 6.97 (1H, d, J = 8.0 Hz, ArH), 6.92 (1H, t, J = 7.6 Hz, ArH), 6.82 (1H, t, J = 7.6 Hz, ArH), 6.44 (1H, d, J = 5.2 Hz, H-3); ^{13}C NMR (100 MHz, $CDCl_3$) δ 184.3 (CHO), 160.6 (CO), 138.5, 137.5, 136.5, 131.2, 130.6, 130.5, 130.0, 129.9, 129.6, 127.4, 127.2, 125.6, 124.8, 124.7, 124.1, 123.5, 123.2, 122.8, 121.7, 121.6, 119.6, 118.4, 117.3, 109.2, 66.1 (CH, C-3), 60.4 (CH, C-4); Anal. Calcd. for $C_{32}H_{22}N_2O_2$: C, 82.38; H, 4.75; N, 6.0. Found: C, 80.93; H, 5.09; N, 6.22.

1-(2-(2-nitrophenyl)-1-(3-nitrophenyl)-4-oxoazetidin-3-yl)-1H-indole-3-carbaldehyde (9k): Pale brown solid, 54%; mp >250 °C; IR (KBr) ν_{max} 1772 (C=O), 1668 (HC=O), 1540 (C−N indole) cm^{-1}; ^1H NMR (400 MHz, $CDCl_3$) δ 9.98 (1H, s, CHO), 8.05 (1H, d, J = 7.6 Hz, ArH), 7.80 (2H, d, J = 8.8 Hz, ArH), 7.72−7.27 (7H, m, ArH), 6.80 (2H, d, J = 8.8 Hz, ArH), 6.70 (1H, d, J = 5.2 Hz, H-4), 5.82 (1H, d, J = 5.2 Hz, H-3); ^{13}C NMR (100 MHz, $CDCl_3$) δ 187.1 (CHO), 162.3 (CO), 157.4, 148.1, 138.8, 136.3, 129.5, 127.6, 124.8, 124.6, 123.7, 123.6, 122.5, 119.2, 118.8, 114.6, 109.0, 69.1 (CH, C-3), 64.3 (CH, C-4); Anal. Calcd. for $C_{24}H_{16}N_4O_6$: C, 63.16; H, 3.53; N, 12.28. Found: C, 64.47; H, 4.33; N, 11.45.

1-(2-(anthracen-9-yl)-1-(4-(diethylamino)phenyl)-4-oxoazetidin-3-yl)-1H-indole-3-carbaldehyde (9l): Yellow solid, 66%; mp 236−239 °C; IR (KBr) ν_{max} 1747 (C=O), 1664 (HC=O), 1515 (C−N indole) cm^{-1}; ^1H NMR (400 MHz, $CDCl_3$) δ 9.44 (1H, s, CHO), 8.67 (1H, d, J = 9.2 Hz, ArH), 8.42 (1H, d, J = 9.2 Hz, ArH), 7.72−7.79 (4H, m, ArH), 8.13 (1H, s, ArH), 7.56 (1H, t, J = 8.0 Hz, ArH), 7.25−7.39 (5H, m, ArH), 6.97 (1H, d, J = 5.2 Hz, H-4), 6.90 (2H, q, J = 7.6 Hz, ArH), 6.77 (1H, t, J = 7.6 Hz, ArH), 6.52 (2H, d, J = 8.8 Hz, ArH), 6.34 (1H, d, J = 5.2 Hz, H-3), 3.25 (4H, q, J = 7.2 Hz, $N(C\underline{H}_2CH_3)_2$), 1.08 (6H, t, J = 7.2 Hz, $N(CH_2C\underline{H}_3)_2$); ^{13}C NMR (100 MHz, $CDCl_3$) δ 184.5 (CHO), 159.3 (CO), 145.8, 138.9, 136.5, 131.2, 130.8, 130.7, 130.6, 130.3, 130.0, 129.7, 127.2, 127.0, 126.6, 124.7, 124.1, 123.7, 123.4, 121.7, 121.6, 120.3, 119.2, 118.2, 112.0, 109.3, 65.8 (CH, C-3), 60.4 (CH, C-4), 44.5 (CH_2, $N(\underline{C}H_2CH_3)_2$), 12.2 ($CH_3$, $N(CH_2\underline{C}H_3)_2$); Anal. Calcd. for $C_{36}H_{31}N_3O_2$: C, 80.42; H, 5.81; N, 7.82. Found: C, 78.85; H, 5.45; N, 7.25.

X-ray crystallography

Single-crystal X-ray diffraction data were obtained at room temperature using a Bruker D8 QUEST diffractometer equipped with Mo Kα radiation and a PHOTON III C14 detector and the data were collected, edited and parameterized by the APEX2 and SAINT. Structure solution and refinement were carried out using SIR2019 [51] and SHELXL-2018 [52], respectively. All H atoms were located in difference maps and then treated as riding atoms. Molecular graphics were created by using OLEX2 [53]. The diffused electron densities were removed by the SQUEEZE routine of PLATON [54].

Anticancer studies

Test procedure and assessment of cell viability

High glucose DMEM medium supplemented with 10% fetal bovine serum (FBS) and 1% (v/v) penicillin-streptomycin was used to grow the cells in a humidified environment with 5% CO_2. Cell survival was investigated by MTT assay. In summary, 1.0×10^4 cells were pre-cultured in each well in a 96-well plate, and after 16 h in the incubator, different concentrations of the complexes (12.5, 25, 50, and 100 μM) were introduced to the cells in a fresh media within 72 h.

Afterwards, each well was treated with fresh medium containing 0.50 mg/ml of MTT solution and incubated for an additional 4 h under the same conditions. The crystalline formazan was dissolved in 100% DMSO by removing the solvent buffer containing culture medium. Spectroscopic measurements were performed on samples by using the BMG Nano Elizabeth reader (570 and 630 nm wavelengths) to determine formazan absorbance and to determine background absorbance, respectively. The percentage of live cells was calculated using the following formula:

$$\text{Cell viability}\% = A_{T(\text{sample})}/A_{T(\text{control})} \times 100$$

where A_T is defined as, $A_{570} - A_{630}$.

The IC_{50} concentration was calculated from three independent experiments using Graph Pad Prism 8 software.

Apoptosis/necrosis analysis

Annexin V is a Ca^{2+}-dependent phospholipid binding protein, with the specific affinity to phosphatidylserine (PS). PS is mainly located on the inner side of the lipid bilayer of normal cell membrane. At the early stages of apoptosis, PS, is flip-floped to the outside, and Annexin V labeled with fluorescent probe dyes (FITC, APC, R-PE fluorescence dyes, and other macromolecules like phycobiliproteins, or biotin as the hapten molecules) is used for specific detection [55]. The accurately of distinguishing viable cells from early or late apoptotic and even necrotic cells can be achieved using DNA intercalating dyes (Propidium iodide (PI), 7-AAD and DAPI). When cells are died with unprogrammed cell death, called necrosis, the cell membrane integrity is interrupted, so the DNA intercalating dyes are capable to penetrate inside the cells and interact with DNA macromolecules. At the early stages of the apoptosis, cells are showing positive fluorescence signals of annexin V-PS, but the membrane integrity is still resists against DNA intercalating dyes. This resistance is lately broken at the late stage of apoptosis.

Annexin V/PI staining was performed using Biolegend's PI/Annexin V apoptosis detection kit. 2×10^5 of HeLa cells were pre-cultured in 24 well plates for 16 h, then the 1xIC50 and 2xIC50 of the compound 4b (21.05 µM and 42.1 µM) and 4o (38.89 µM and 77.78 µM) were tested for 24 h at 37 °C. Then, the cells were washed twice with 1 ml of phosphate-buffered saline (PBS), then once with 1 ml of binding buffer (containing Ca^{2+} for specific interaction of Annexin to phosphatidyl serine). The washed cells were then suspended for 15 min in 100 µl of binding buffer containing 5 µl of Annexin V-FITC and 5 µl of Propodium Iodide (PI). After washing again with binding buffer, the cells were resuspended in 400 µl of the same buffer. Apoptosis rates were subsequently determined by FACS CaliburTM flow cytometry (BD Bioscience, San Jose, CA, USA).

In vitro anti-inflammatory studies

Principle of the assay

The in vitro anti-inflammatory assay is based on the ability of macrophages to generate a strong inflammatory response when stimulated with antigens. Mouse immortalized macrophages are stimulated by *E. coli* LPS, and exposed to the test material for 24 h. At the end of the incubation period, NO production is evaluated indirectly by measuring the accumulation of nitrite/nitrate, the stable end-products of NO oxidation, in the culture medium using a spectrophotometric method based on the Griess reaction.

Cell line: mouse macrophages (RAW 264.7, Sigma-Aldrich, No. P6110401, Lot. 09I006), low passage number (<50).

Culture medium: DMEM with stable L-glutamine (Dulbecco's Minimum Essential Medium) supplemented with Penicillin 100 IU/ml and streptomycin 100 µg/ml and 10% of inactivated calf serum with pH 7.2, freshly prepared, stored no longer than 3 weeks.

Diluent: Dimethyl sulfoxide (DMSO).

Negative control: DMSO.

Positive control: Dexamethasone (1−5−10−50−100 µM).

Test procedure

Cells were seeded into 48-well tissue culture plates at a concentration of 1×10^5 cells/ml (200 µl/well) and maintained for 24 h at 37 °C (5% CO_2). The culture medium was then replaced by 200 µl of medium containing different concentrations of the test compounds. The cells were incubated at 37 °C (5% CO_2) for 1 h. Pro-inflammatory LPS from *E. coli* was then added to the cell cultures (1 µg/ml) and the cells were incubated at 37 °C (under 5% CO_2) for 24 h.

Assessment of NO release

NO release in the culture supernatant was measured by the Griess reaction. In total, 100 µl of the supernatants from the test procedure above were transferred into the wells of a 96-well tissue culture plate, and 100 µl of the Griess modified reagent were added in each well. The Optical Density (OD) of each well was read by a fluorescence-luminescence reader Infinite M200 Pro (TECAN) at 540 nm, after a 15 min at room temperature. The results for wells that were treated with test compound were compared to those of the untreated wells (DMSO, 100% viability) and converted to percentage values.

Assessment of cell viability

Cell viability was measured in parallel to the assessment of NO release, to validate the assay. WST-1 vital dye reagent

was used to determine cell mitochondrial respiration. In this meant, the culture medium was decanted and WST-1 reagent (100 µl, 1/10 dilution) was added in each well. The Optical Density (OD) of each well, after a 30-min incubation period at 37 °C (5% CO_2), was read at 450 nm by a fluorescence-luminescence reader Infinite M200 Pro (TECAN) spectrometer. The results for wells treated with the test material were compared to those of untreated control wells (DMSO, 100% viability) and converted to percentage values.

Calculation of the IC_{50}

NO release inhibition and cell viability inhibition are expressed as percentages as compared to the negative controls:

$$\text{Percentage of NO release} = \frac{100\times(\text{OD of test well} - \text{OD of blank})}{\text{OD of DMSO control} - \text{OD of blank}}$$

$$\text{Percentage of Cell viability} = \frac{100\times(\text{OD of test well} - \text{OD of blank})}{\text{OD of DMSO control} - \text{OD of blank}}$$

Software Tablecurve Version 2.0 was used to calculate the concentrations of the test material causing respectively a 50% decrease of NO release ($IC_{50\text{-NO release}}$) and a 50% decrease of cell viability ($IC_{50\text{-cell viability}}$). The ratio between the anti-inflammatory activity and the toxicity is expressed as anti-inflammatory ratio. It is calculated as follows:

$$\text{Anti-inflammatory ratio} = IC_{50\text{-cell viability}}/IC_{50\text{-NO release}}$$

Molecular docking studies

Because of the various 3D-structures available for human nitric oxide synthase, docking validation was implemented to identify an appropriate X-ray structure for docking simulations. Several PDB codes were chosen from the Protein Data Bank website (http://www.rcsb.org) to find the ideal starting model for human nitric oxide synthase. All the PDB codes obtained were subjected to a self-docking validation test. This involved redocking cognate ligands on their corresponding 3D structures and superimposing the best docking poses with the native conformation of the ligand in the crystallographic state. The 4nos PDB code was selected from the PDB files based on the root-mean-square deviation (RMSD) value. The synthesized compounds were sketched, energy minimized, and saved in pdbqt format as ligand molecules. To prepare the protein for docking simulation, all co-crystallized ligands and water molecules were removed while the missing hydrogens were added. Non-polar hydrogens were merged with their corresponding carbons, and the protein was converted into the required pdbqt format. Auto Dock Tools package (1.5.6) was used for all preparation procedures. Finally, docking simulations were performed using bash scripting in a Linux operating system. Docking was performed using Autodock Vina (1.1.2) within a defined box, determined by the following parameters. The grid box had a size of 30 × 30 × 30 and was centered on the co-crystallized ligand. The coordinates for the center of the grid box were determined as [x = 10.889, y = 97.563, z = 11.383] for the 4nos pdb code. Exhaustiveness was set at 100, while the other docking parameters were left at the default settings. Following the docking simulations, the best docking poses were subsequently selected for further analysis of the interactions between the enzyme and the inhibitor [56].

Supplementary information The online version contains supplementary material available at https://doi.org/10.1007/s00044-023-03152-5.

Acknowledgements We appreciate the financial support from Shiraz University Research Council (Grant No. 99-GR-SC-23); Shiraz University of Medical Science for anticancer studies; Sinop University, Turkey, for the use of the Bruker D8 QUEST diffractometer and Centre de Recherche en Cancérologie de Marseille, France for anti-inflammatory studies.

Compliance with ethical standards

Conflict of interest The authors declare no competing interests.

References

1. Salunkhe DS, Piste PB. A brief review on recent synthesis of 2-azetidinone derivatives. Int J Pharm Sci Res. 2014;5:666−89. https://doi.org/10.13040/IJPSR.0975-8232.5(3).666-89.
2. Mermer A, Bayrak H, Alyar S, Alagumuthu M. Synthesis, DFT calculations, biological investigation, molecular docking studies of β-lactam derivatives. J Mol Struct. 2020;1208:127891. https://doi.org/10.1016/j.molstruc.2020.127891.
3. Zhang H, Lv X, Yu H, Bai Z, Chen G, He G. β-Lactam synthesis via copper-catalyzed directed aminoalkylation of unactivated alkenes with cyclobutanone O-benzoyloximes. Org Lett. 2021;23:3620−25. https://doi.org/10.1021/acs.orglett.1c01007.
4. Farhan MM, Guma MA, Rabeea MA, Ahmad I, Patel H. Synthesizes, characterization, molecular docking and in vitro bioactivity study of new compounds containing triple beta lactam rings. J Mol Struct. 2020;1269:133781. https://doi.org/10.1016/j.molstruc.2022.133781.
5. Paniagua A, Yadav RN, Hossain MF, Srivastava AK, Banik BK. A novel synthesis of densely functionalized 3,4-β-lactam fused 1,4-oxazepane via tandem-7-exo-trig intramolecular oxa-michael reaction. Mosc Univ Chem Bull. 2022;77:117−24. https://doi.org/10.3103/S0027131422020080.
6. Jarrahpour A, Zarei M. Synthesis of novel *N*-sulfonyl monocyclic β-lactams as potential antibacterial agents. Molecules. 2006;11:49−58. https://doi.org/10.3390/11010049.
7. Mishra MK, Singh VN, Ahmad K, Sharma S. Synthesis and antimicrobial activities of some novel diastereoselective monocyclic cis-β-lactams using 2-ethoxy carbonyl DCPN as a carboxylic acid activator. Mol Divers. 2021;25:2073−87. https://doi.org/10.1007/s11030-020-10099-x.
8. Galletti P, Giacomini D. Monocyclic β-lactams: new structures for new biological activities. Curr Med Chem. 2011;18:4265−83. https://doi.org/10.2174/092986711797200480.

9. Kamath A, Ojima I. Advances in the chemistry of β-lactam and its medicinal applications. Tetrahedron. 2012;68:10640−64. https://doi.org/10.1016/j.tet.2012.07.090.
10. Kristensen PJ, Gegelashvili G, Munro G, Heegaard AM, Bjerrum OJ. The β-lactam clavulanic acid mediates glutamate transport-sensitive pain relief in a rat model of neuropathic pain. Eur J Pain. 2018;22:282−94. https://doi.org/10.1002/ejp.1117.
11. Alborz M, Jarrahpour A, Pournejati R, Karbalaei-Heidari HR, Sinou V, Latour C, et al. Synthesis and biological evaluation of some novel diastereoselective benzothiazole β-lactam conjugates. Eur J Med Chem. 2018;143:283−91. https://doi.org/10.1016/j.ejmech.2017.11.053.
12. Ranjbari S, Behzadi M, Sepehri S, Dadkhah AM, Jarrahpour A, Mohkam M, et al. Investigations of antiproliferative and antioxidant activity of β-lactam morpholino-1,3,5-triazine hybrids. Bioorg Med Chem. 2020;28:115408. https://doi.org/10.1016/j.bmc.2020.115408.
13. Xinfen Z, Yanshu J. Recent advances in β-lactam derivatives as potential anticancer agents. Curr Top Med Chem. 2020;20:1468−80. https://doi.org/10.2174/1568026620666200309161444.
14. Nagarajan S, Arjun P, Raaman N, Shah A, Sobhia ME, Das TM. Stereoselective synthesis of sugar-based β-lactam derivatives: docking studies and its biological evaluation. Tetrahedron. 2012;68:3037−45. https://doi.org/10.1016/j.tet.2012.02.017.
15. Borazjani N, Sepehri S, Behzadi M, Jarrahpour A, Ameri Rad J, Sasanipour M, et al. Three-component synthesis of chromeno β-lactam hybrids for inflammation and cancer screening. Eur J Med Chem. 2019;179:389−403. https://doi.org/10.1016/j.ejmech.2019.06.036.
16. Bhati SK, Kumar A. Synthesis of new substituted azetidinoyl and thiazolidinoyl-1,3,4-thiadiazino (6,5-b) indoles as promising anti-inflammatory agents. Eu J Med Chem. 2008;43:2323−30. https://doi.org/10.1016/j.ejmech.2007.10.012.
17. O'Driscoll M, Greenhalgh K, Young A, Turos E, Dickey S, Lim DV. Studies on the antifungal properties of N-thiolated β-lactams. Bioorg Med Chem. 2008;16:7832−37. https://doi.org/10.1016/j.bmc.2008.06.035.
18. Thanikachalam PV, Maurya RK, Garg V, Monga V. An insight into the medicinal perspective of synthetic analogs of indole. Eur J Med Chem. 2019;183:562−612. https://doi.org/10.1016/j.ejmech.2019.111680.
19. Lamie PF, Ali WAM, Bazgier V, Rárová L. Novel *N*-substituted indole Schiff bases as dual inhibitors of cyclooxygenase-2 and 5-lipoxygenase enzymes: synthesis, biological activities in vitro and docking study. Eur J Med Chem. 2016;123:803−13. https://doi.org/10.1016/j.ejmech.2016.08.013.
20. Dousson C, Alexandre FR, Amador A, Bonaric S, Bot S, Caillet C, et al. Standring, discovery of the aryl-phospho-indole IDX899, a highly potent anti-HIV non-nucleoside reverse transcriptase inhibitor. J Med Chem. 2016;59:1891−8. https://doi.org/10.1021/acs.jmedchem.5b01430.
21. Stec J, Onajole OK, Lun S, Guo H, Merenbloom B, Vistoli G, et al. Indole-2-carboxamide-based MmpL3 inhibitors show exceptional antitubercular activity in an animal model of tuberculosis infection. J Med Chem. 2016;59:6232−47. https://doi.org/10.1021/acs.jmedchem.6b00415.
22. Yadav RR, Khan SI, Singh S, Khan IA, Vishwakarma RA, Bharate SB. Synthesis, antimalarial and antitubercular activities of meridianin derivatives. Eur J Med Chem. 2015;98:160−9. https://doi.org/10.1016/j.ejmech.2015.05.020.
23. Praveen C, Ayyanar A, Perumal PT. Practical synthesis, anticonvulsant, and antimicrobial activity of *N*-allyl and *N*-propargyl di(indolyl)indolin-2-ones. Bioorg Med Chem Lett. 2011;21:4072−77. https://doi.org/10.1016/j.bmcl.2011.04.117.
24. Nomura S, Yamamoto Y, Matsumura Y, Ohba K, Sakamaki S, Kimata H, et al. Novel indole-*N*-glucoside, TA-1887 as a sodium glucose cotransporter 2 inhibitor for treatment of type 2 diabetes. ACS Med Chem Lett. 2014;5:51−5. https://doi.org/10.1021/ml400339b.
25. Gomha SM, Riyadh SM. Synthesis under microwave irradiation of [1,2,4]Triazolo[3,4-b] [1,3,4]thiadiazoles and other diazoles bearing indole moieties and their antimicrobial evaluation. Molecules. 2011;16:8244−56. https://doi.org/10.3390/molecules16108244.
26. Weng JR, Tsai CH, Kulp SK, Chen CS. Indole-3-carbinol as a chemopreventive and anti-cancer agent. Cancer Lett. 2008;262:153−63. https://doi.org/10.1016/j.canlet.2008.01.033.
27. Estevão MS, Carvalho LC, Ribeiro D, Couto D, Freitas M, Gomes A, et al. Antioxidant activity of unexplored indole derivatives: synthesis and screening. Eur J Med Chem. 2010;45:4869−78. https://doi.org/10.1016/j.ejmech.2010.07.059.
28. Fahima AM, Farag AM, Mermer A, Bayrak H, Sirin Y. Synthesis of novel β-lactams: antioxidant activity, acetylcholinesterase inhibition and computational studies. J Mol Struct. 2021;1233:130092. https://doi.org/10.1016/j.molstruc.2021.130092.
29. Zhang MZ, Jia CY, Gu YC, Mulholland N, Turner S, Beattie D, et al. Synthesis and antifungal activity of novel indole-replaced streptochlorin analogues. Eur J Med Chem. 2017;126:669−74. https://doi.org/10.1016/j.ejmech.2016.12.001.
30. Rajan S, Puri S, Kumar D, Babu MH, Shankar K, Varshney S, et al. Novel indole and triazole based hybrid molecules exhibit potent anti-adipogenic and antidyslipidemic activity by activating Wnt3a/β-catenin pathway. Eur J Med Chem. 2018;143:1345−60. https://doi.org/10.1016/j.ejmech.2017.10.034.
31. Mohamadzadeh M, Zarei M, Vessal M. Synthesis, in vitro biological evaluation and in silico molecular docking studies of novel β-lactam-anthraquinone hybrids. Bioorg Chem. 2020;95:103515. https://doi.org/10.1016/j.bioorg.2019.103515.
32. Raju R, Raghunathan R, Arumugam N, Almansour AI, Kumar RS. Regio- and stereoselective synthesis of novel β-lactam engrafted spiroheterocyclic hybrids via one-pot three component cycloaddition strategy. Tetrahedron Lett. 2020;61:152661. https://doi.org/10.1016/j.tetlet.2020.152661.
33. Raju R, Raghunathan R, Arumugam N, Almansour AI, Kumar RS, Soliman SM. Stereo- and regioselective synthesis of novel β-lactam tethered spiropyrrolizidine/pyrrolothiazole heterocyclic hybrids. Tetrahedron. 2021;84:132026. https://doi.org/10.1016/j.tet.2021.132026.
34. Dhawan S, Awolade P, Kisten P, Cele N, Pillay AS, Saha ST, et al. Synthesis, cytotoxicity and antimicrobial evaluation of new coumarin-tagged β-lactam triazole hybrid. Chem Biodivers. 2020;17:1900462. https://doi.org/10.1002/cbdv.201900462.
35. Borazjani N, Jarrahpour A, Ameri Rad J, Mohkam M, Behzadi M, Ghasemi Y, et al. Design, synthesis and biological evaluation of some novel diastereoselective β-lactams bearing 2-mercaptobenzothiazole and benzoquinoline. Med Chem Res. 2019;28:329−39. https://doi.org/10.1007/s00044-018-02287-0.
36. Ameri Rad J, Jarrahpour A, Ersanl CC, Atioglu Z, Akkurt M, Turos E. Synthesis of some novel indeno[1,2-b]quinoxalin spiro-β-lactam conjugates. Tetrahedron. 2017;73:1135−42. https://doi.org/10.1016/j.tet.2017.01.009.
37. Jarrahpour A, Heiran R, Sinou V, Latour C, Bouktab LD, Brunel JM, et al. Synthesis of new β-lactams bearing the biologically important morpholine ring and POM analyses of their antimicrobial and antimalarial activities. Iran J Pharm Res. 2019;18:34−48. https://doi.org/10.22037/ijpr.2019.2348.
38. Jarrahpour A, Jowkar Z, Haghighijoo Z, Heiran R, Ameri Rad J, Sinou V, et al. Synthesis, in-vitro biological evaluation, and molecular docking study of novel spiro-β-lactam-isatin hybrids. Med Chem Res. 2022;31:1026−34. https://doi.org/10.1007/s00044-022-02898-8.

39. Soto S, Vaz E, Aversana CD, Álvarez R, Altucci L, Lera ARD. New synthetic approach to paullones and characterization of their SIRT1 inhibitory activity. Org Biomol Chem. 2012;10:2101−12. https://doi.org/10.1039/C2OB06695E.
40. Allen FH, Kennard O, Watson DG, Brammer L, Orpen AG, Taylor R. Tables of bond lengths determined by X-ray and neutron diffraction. Part 1. Bond lengths in organic compounds. J Chem Soc Perkin Trans II. 1987;12:S1−19. https://doi.org/10.1039/P298700000S1.
41. Akkurt M, Karaca S, Jarrahpour A, Khalili D, Büyükgüngör O. 3-phenoxy-1,4-diphenylazetidin-2-one. Acta Crystallogr Sect E Crystallogr Commun. 2006;62:o866−8. https://doi.org/10.1107/S160053680600314X.
42. Akkurt M, Karaca S, Jarrahpour A, Zarei M, Büyükgüngör O. 2-[1-(4-Ethoxyphenyl)-2-oxo-4-styrylazetidin-3-yl]isoindoline-1,3-dione. Acta Crystallogr Sect E Crystallogr Commun. 2008;64:o924. https://doi.org/10.1107/S1600536808011586.
43. Akkurt M, Türktekin S, Jarrahpour A, Badrabady SAT, Büyükgüngör O. 3-(2,4-Dichlorophenoxy)-1-(4-methoxyphenyl)-4-(3-nitrophenyl)azetidin-2-one. Acta Crystallogr Sect E Crystallogr Commun. 2010;67:o183. https://doi.org/10.1107/S1600536810052645.
44. Atioğlu Z, Akkurt M, Jarrahpour A, Heiran R, Özdemir N. 1-[3-(Morpholin-4-yl)propyl]-3-[(naphthalen-2-yl)oxy]-4-(3-nitrophenyl)azetidin-2-one. Acta Crystallogr Sect E Crystallogr Commun. 2014;70:o833−4. https://doi.org/10.1107/S1600536814014949.
45. Atioğlu Z, Akkurt M, Jarrahpour A, Heiran R, Özdemir N. 3-(2,4-Dichlorophenoxy)-1-(4-methoxybenzyl)-4-(4-nitrophenyl)azetidin-2-one. Acta Crystallogr Sect E Crystallogr Commun. 2014;70:o835−6. https://doi.org/10.1107/S1600536814015013.
46. Bernstein J, Davis RE, Shimoni L, Chang NL. Patterns in hydrogen bonding: functionality and graph set analysis in crystals. Angew Chem Int Ed. 1995;34:1555−73. https://doi.org/10.1002/anie.199515551.
47. Poderoso JJ, Carreras MC, Lisdero C, Riobo N, Schopfer F, Boveris A. Nitric oxide inhibits electron transfer and increases superoxide radical production in rat heart mitochondria and submitochondrial particles. Arch Biochem Biophys. 1996;328:85−92. https://doi.org/10.1006/abbi.1996.0146.
48. Seo YH, Kim JK, Jun JG. Synthesis and biological evaluation of piperlongumine derivatives as potent anti-inflammatory agents. Bioorg Med Chem Lett. 2014;24:5727−30. https://doi.org/10.1016/j.bmcl.2014.10.054.
49. Cinelli MA, Do HT, Miley GP, Silverman RB. Inducible nitric oxide synthase: regulation, structure, and inhibition. Med Res Rev. 2020;40:158−89. https://doi.org/10.1002/med.21599.
50. Heiran R, Sepehri S, Jarrahpour A, Digiorgio C, Douafer H, Brunel JM, et al. Synthesis, docking and evaluation of in vitro anti-inflammatory activity of novel morpholine capped β-lactam derivatives. Bioorg Chem. 2020;102:104091. https://doi.org/10.1016/j.bioorg.2020.104091.
51. Burla MC, Caliandro R, Carrozzini B, Cascarano GL, Cuocci C, Giacovazzo C, et al. Crystal structure determination and refinement via SIR2014. J Appl Crystallogr. 2015;48:306−9. https://doi.org/10.1107/S1600576715001132.
52. Sheldrick GM. Crystal structure refinement with SHELXL. Acta Crystallogr Sect C Struct Chem. 2015;71:3−8. https://doi.org/10.1107/S2053229614024218.
53. Dolomanov OV, Bourhis LJ, Gildea RJ, Howard JAK, Puschmann H. OLEX2: a complete structure solution, refinement and analysis program. J Appl Crystallogr. 2009;42:339−41. https://doi.org/10.1107/S0021889808042726.
54. Spek AL. Structure validation in chemical crystallography. Acta Crystallogr Sect D Struct Biol. 2009;65:148−55. https://doi.org/10.1107/S090744490804362X.
55. Logue SE, Elgendy M, Martin SJ. Expression, purification and use of recombinant annexin V for the detection of apoptotic cells. Nat Protoc. 2009;4:1383−95. https://doi.org/10.1038/ nprot.2009.143.
56. Riazimontazer E, Sadeghpour H, Nadri H, Sakhteman A, Küçükkılınç TT, Miri R, et al. Design, synthesis and biological activity of novel tacrine-isatin Schiff base hybrid derivatives. Bioorg Chem. 2019;89:103006. https://doi.org/10.1016/j.bioorg.2019.103006.